Master's Thesis
Synthetic Chemistry

Mechanochemical synthesis of functionalized phthalocyanine precursors by nucleophilic aromatic substitution

Obed Rodriguez-Perez

April 28, 2025

Supervisor(s): PhD. Eduardo Anaya-Plaza
Assoc. Prof. PhD. Filip Ekholm

UNIVERSITY OF HELSINKI
FACULTY OF SCIENCE
Master's Programme in Chemistry and Molecular Sciences

PL 64 (Gustaf Hällströmin katu 2a)
FI-00014

HELSINGIN YLIOPISTO — HELSINGFORS UNIVERSITET — UNIVERSITY OF HELSINKI

Tiedekunta — Fakultet — Faculty	Koulutusohjelma — Utbildningsprogram — Education programme
Faculty of Science	Master's Programme in Chemistry and Molecular Sciences

Tekijä — Författare — Author
Obed Rodriguez-Perez

Työn nimi — Arbetets titel — Title
Mechanochemical synthesis of functionalized phthalocyanine precursors by nucleophilic aromatic substitution

Opintosuunta — Studieinriktning — Study track
Synthetic Chemistry

Työn laji — Arbetets art — Level	Aika — Datum — Month and year	Sivumäärä — Sidoantal — Number of pages
Master's Thesis	April 28, 2025	64 pages

Tiivistelmä — Referat — Abstract

Phthalocyanines are a prominent class of organic dyes known for their remarkable photochemical and photophysical properties, making them valuable in a wide range of applications, from photodynamic therapy to solar energy conversion. Functionalization of these compounds is particularly important, as it enables the precise tuning of their properties for specific uses. Among the various methods available for synthesizing functionalized phthalocyanines, the nucleophilic aromatic substitution (S_NAr) of phthalonitrile precursors stands out as one of the most versatile and widely employed, owing to the broad availability of starting materials and the adaptability of the reaction.

However, the traditional synthesis of phthalocyanines often relies heavily on polar aprotic solvents and elevated temperatures, contributing to significant environmental impact. To address these concerns and move toward more sustainable practices in organic synthesis, mechanochemistry has emerged as a promising alternative. This solvent-minimizing methodology utilizes mechanical force to drive chemical transformations, offering a greener approach by significantly reducing both solvent consumption and reaction times.

Although mechanochemical S_NAr reactions have garnered attention in recent years, their application to the synthesis of phthalocyanine precursors remains unexplored. In this work, we aimed to assess the feasibility of this approach, systematically optimize the reaction conditions, and evaluate the robustness and versatility of the methodology. Additionally, the study was extended to a preliminary investigation into the tetramerization of the resulting precursors, providing early insights into the potential for a fully mechanochemical synthesis of functionalized phthalocyanines. Lastly, our approach was briefly compared to conventional solvent-based methods and its strengths and limitations were assessed.

Avainsanat — Nyckelord — Keywords
phthalocyanines, phthalonitriles, mechanochemistry, nucleophilic aromatic substitution, LAG

Säilytyspaikka — Förvaringsställe — Where deposited
E-thesis, Kumpula Campus Library, Department of Chemistry

Muita tietoja — övriga uppgifter — Additional information

Contents

List of abbreviations

DBU	=	1,8-diazabicyclo[5.4.0]undec-7-ene
DMAE	=	2-dimethylaminoethanol
DMF	=	*N,N*-dimethylformamide
DMSO	=	dimethylsulfoxide
ESI	=	electrospray ionization
EWG	=	electron-withdrawing group
LAG	=	liquid-assisted grinding
LG	=	leaving group
MALDI-TOF	=	matrix-assisted laser desorption/ionization-time of flight
NMR	=	nuclear magnetic resonance
S_NAr	=	nucleophilic aromatic substitution
THF	=	tetrahydrofuran
TLC	=	thin-layer chromatography
η	=	liquid-to-solid ratio (mg/µL)

1. Introduction

Phthalocyanines are a class of organic dyes formed by four isoindole units linked by nitrogen atoms in a macrocycle often featuring a metallic center (**Figure 1.1**). Their planar geometry and 18-electron delocalized system endow these molecules with a vast array of photochemical and photophysical properties affording them interesting applications in areas ranging from photovoltaics to biosensing and photodynamic therapy.[1;2;3] Their useful properties are attributed to their efficient electron transfer abilities[4] and their relative ease of functionalization, which enhances their applications by finely tuning their photochemical properties and extending the range of wavelength absorption.[5] The versatility of phthalocyanines has been attested in a number of literature reviews and scientific publications.[3;5;6]

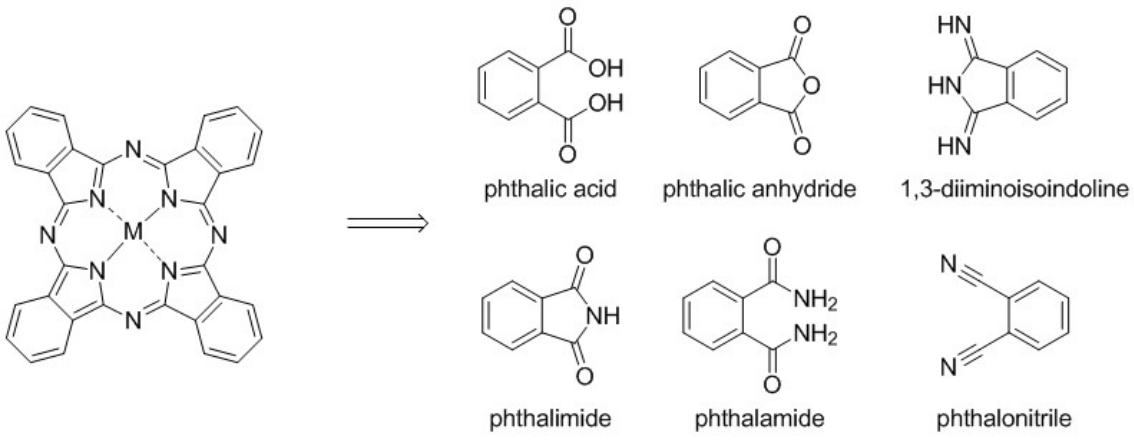

Figure 1.1: Phthalocyanine with retrosynthetic analysis (M = metal).

The synthesis of functionalized phthalocyanines from phthalic acid derivatives and

phthalonitriles is a robust and reliable method to afford these pigments. Usually, functionalized phthalonitriles or phthalimides can be prepared, affording desired substituted precursors to be used in the preparation of phthalocyanines.[6] An alternative approach consists of the modification of already existing functionalized phthalocyanines by different means, although this alternative remains limited to soluble phthalocyanines. The insolubility of symmetrical phthalocyanines remains a practical challenge for their postfunctionalization.

Among the number of reactions developed for phthalonitriles, nucleophilic aromatic substitution (S_NAr) is a favoured one given the rich chemistry, availability of nucleophiles and cheap selection of electrophiles. However, nucleophilic aromatic substitution is largely reliant on the use of polar aprotic solvents and long reaction times,[7] whereas the tetramerization reaction is typically energy intensive, requiring heating at temperatures ranging from 130 to 250 °C and large amounts of solvents such as 2-dimethylaminoethanol (DMAE) and *N,N*-dimethylformamide (DMF). Thus, more environmentally friendly alternatives are to be desired to lower the environmental impact of the synthesis.

In recent years, synthetic methodologies hav been designed to lower the energy input of the reaction with the use of alternatives such as microwave and ultraviolet radiation; and different reaction media such as ionic liquids and solid-state synthesis.[6] The latter remains a largely underdeveloped area in chemical synthesis despite its potential. The main goal of solid-state synthesis is to reduce the quantities of solvent used to the minimal amount possible, employing mechanical forces to drive the reaction. It relies on mechanochemistry and heating for its energy input with the potential of lowering the environmental impact of the synthetic procedure. The mechanochemical approach to phthalocyanines has been regarded as largely under-

explored in the literature concerning these dyes.[6]

The aim of this thesis is thus to explore and evaluate the functionalization of phthalocyanine precursors by nucleophilic aromatic substitution through mechanochemical and solid-state means. In this work, the nucleophilic aromatic substitution of phthalocyanine precursors was optimized by screening through different reaction conditions. The optimized results were then applied to a range of nucleophiles and phthalonitrile substrates that provided functionalization of interest. The tetramerization of a few synthesised precursors by mechanochemistry-aided aging was briefly explored.

2. Theoretical background

In this chapter, we will explore the relevant connections between mechanochemistry and nucleophilic aromatic substitution and the independent interaction of each with the synthesis of functionalized phthalocyanines. This will be supported with relevant literature examples that will highlight the work currently done on the field allowing us to gain a deeper understanding on the reasons and goals of this work.

2.1 Synthesis of phthalocyanines

2.1.1 Traditional methods

Phthalocyanines are planar aromatic molecules that have generated interest in the scientific community due to their exceptional chemical, electronic and optical properties. Furthermore, the α- and β- positions in the macrocycle can be widely functionalized to meet specific photochemical properties as needed. Accidentally discovered in the beginning of the 20th century,[8] they were not fully characterized until the 1930's[9] after which they have been widely used in the pigment industry.

The synthesis of the phthalocyanine ring typically occurs via a cyclocondensation reaction usually involving phthalic acid derivatives, 1,3-diiminisoindole and phthalonitriles, the latter of which are the most used at the laboratory scale and the subject of our research (**Figure 2.1**).[6]

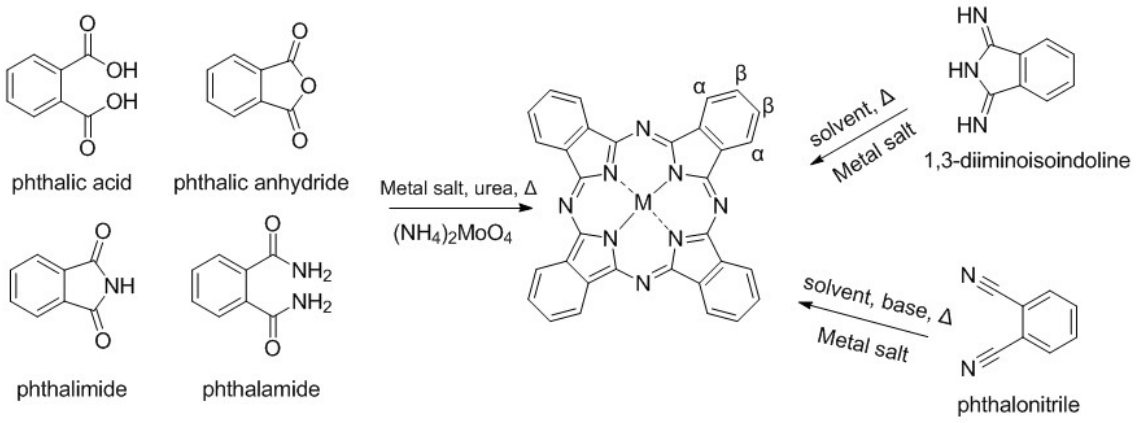

Figure 2.1: Common synthetic routes for the preparation of phthalocyanines. Modified from [6].

The macrocyclization reaction typically occurs at high thermal conditions in solvents such as DMF,[10] DMAE,[11] quinoline[12] or pentanol,[13] and it can be catalysed by a non-nucleophilic base like 1,8-diazabicyclo[5.4.0]undec-7-ene (DBU)[14] or a lithium alkoxide generated in-situ.[15] If a metallic center is desired, a metal template is used, typically in the +2 oxidation state, significantly aiding the tetramerization in detriment of side reactions due to the perfect fit between the ionic radius of the metal and the inner space within the macrocycle.[6]

2.1.2 Sustainable synthesis

In recent years, alternative methods have emerged as part of the collective efforts to address the environmental impact of chemical synthesis. The synthesis of phthalocyanines is an energy intensive process that requires heat and produces waste in the form of organic solvents. As such, it has started to be the target of alternative methodologies based on alternative energy inputs or reaction media, although discussion about the environmental footprint of the reaction has been limited until very recently.[16]

The use of energy inputs such as ultrasound,[17] UV[18] and microwave irradiation[19] is well documented, as well as the attempted reduction of solvent impact in the use of benign solvents,[20] ionic liquids[21] and deep eutectic solvents.[22] The use of solid-state synthesis and mechanochemical methods for the synthesis of phthalocyanines has been documented by our research group.

Solvent-free phthalocyanine synthesis has been described at the molten state, usually in temperatures over 160 °C. For phthalic precursors, urea is typically employed in its molten state as a solvent and nitrogen source as reported by Zhu et al.[23] in their synthesis of sulfonated cobalt phthalocyanines. For phthalonitriles, urea has been also employed for the solid-state synthesis of alkylthio-substituted titanyl phthalocyanine by McGrath et al., with yields ranging from 30-40%,[24] whereas Wu et al. has reported the synthesis of a cobalt nitrophthalocyanine following a similar procedure.[25]

Lokesh and Adriaens have reported the synthesis of tetrasubstituted palladium phthalocyanine complexes in the solid-state. Especially remarkable is their tetranitrophthalocyanine preparation in which the nitrophthalonitrile and the metal templating agent are stirred in a slurry state at 160 °C, although specific yields are not reported due to possible contamination by impurities arising from phthalocyanine oligomerization as suggested by small discrepancies in the characterization.[26]

A more mechanochemical approach has been explored in our research group by combining liquid-assisted mechanochemistry with aging in the solid-state synthesis of tetra-*tert*-butylphthalocyanines (**Scheme 1**). In this work, the phthalonitrile and metal salt would be pre-milled with a small amount of DMAE (liquid-to solid ratio

(η) = 0 - 0.192 µL/mg) and then aged in the oven at a 100 °C for 48 hours. Different parameters were optimized but the most influential seemed to be the liquid to solid ratio and the aging temperature. The presence of DMAE acted as nucleophilic catalyst in the initial stages, whereas the aging temperature aided the mixture of the reactants at a transition state near melting. In optimal conditions, conversions up to 99% were achieved in 48 hours and the scalability was tested successfully withouth affecting the conversion, which is remarkable in laboratory settings.[27] The phthalocyanine synthesis in the present work is largely derived from the optimized conditions in this article.

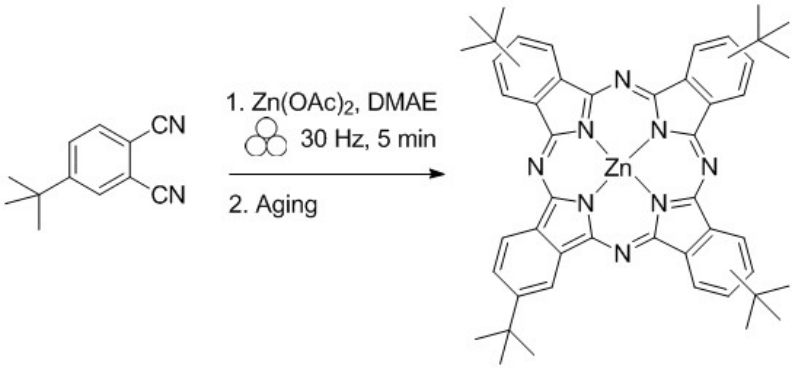

Scheme 1: Mechanochemically-aided phthalocyanine synthesis by our group.[27]

Recently, Fan et al. also reported a mechanochemical approach to the synthesis of phthalocyanine scaffolds for energy storage, affording polymeric materials of variable porosity and high surface area in moderate yields.[28]

The mechanochemical approach to phthalocyanines has an untapped potential that could allow for access to a range of materials that would be otherwise difficult to obtain due to the sometimes extremely low solubility of these macromolecules. Furthermore, it could open the door to ample functionalization, broadening the range of properties even further.

2.1.3 Functionalization of phthalocyanines

The functionalization of phthalocyanines by introducing peripheral substituents can dramatically alter their solubility in water and organic solvents; and can be used to accurately tune the optical and redox properties of the synthesized phthalocyanines.[29] The two basic synthetic routes consist of a pre- or a post-functionalization of the phthalocyanine moiety. In the pre-functionalization approach, phthalic acid derivatives and phthalonitriles are functionalized with the desired functional groups before the tetramerization occurs. This approach is by far the most popular one due to the prevalence of cheap and commercially available starting materials and the many possibilities offered by known synthetic strategies for the addition of functional groups to these molecules. The second approach, largely underexplored, relies on the tetramerization of a substituted phthalonitrile before the addition of the desired product, often by nucleophilic or electrophilic aromatic substitution (**Figure 2.2**).

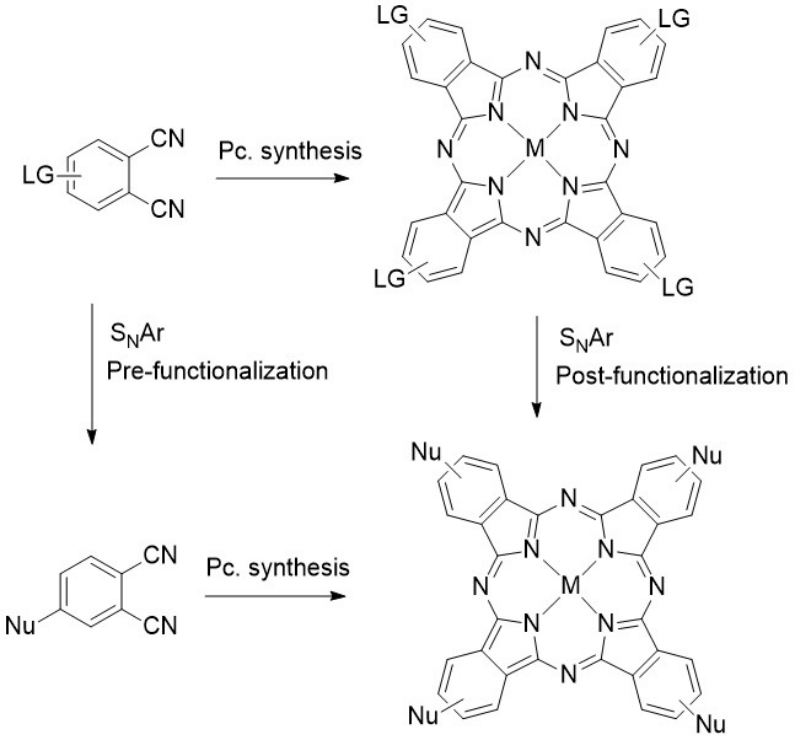

Figure 2.2: Phthalocyanine functionalization strategies. Modified from [50].

Pre-functionalization approach

The pre-functionalization approach to phthalocyanines peripheral substitution has been thoroughly reviewed,[30;31] affording the preparation of alkyl,[32] aryl,[33] nitro,[34] halogen,[35] oxy[36] and thio-[37] substituted phthalocyanines with a wide range of properties. The tetramerization of substituted phthalonitriles is the most common approach to tetrasubstituted phthalocyanines,[31] and as such it has been the model for our mechanochemical synthesis.

Nucleophilic aromatic substitution (S_NAr) is a type of substitution reaction in which a nucleophile replaces a leaving group, typically a halogen, on an aromatic ring. The use of S_NAr in the functionalization of phthalonitriles has been widely reported in the previously cited reviews as one of the most convenient ways to introduce electron-donating groups to phthalocyanines from nitro- or bromo-substituted phthalonitriles. This method has been the subject of rich literature on the functionalization of phthalocyanines and the interest has arisen from the versatility of phthalonitrile derivatives for the introduction of moieties of extreme diversity.[31]

Some recent examples that showcase the vitality of this approach are the synthesis of novel methoxyphenylthio-substituted phthalocyanines for acid-sensing properties by Odabas et al., applying nucleophilic aromatic substitution of 3- or 4-nitrophthalonitrile with relevant substituted thiol, after which tetramerization afforded the desired phthalocyanines in low to moderate yields (30-60%) (**Scheme 2**).[38] The reaction conditions for substitution were typical, using DMF as a solvent with reaction times ranging from 24-48 hours, while the tetramerization made use of lithium alkoxide with amyl alcohol in a 5 ml/mmol ratio to the phthalonitrile. Thymoxy-substituted phthalocyanines with redox applications have been synthesized in a similar approach by Odabas et al., with a DBU catalysed tetrameriza-

tion.[39]

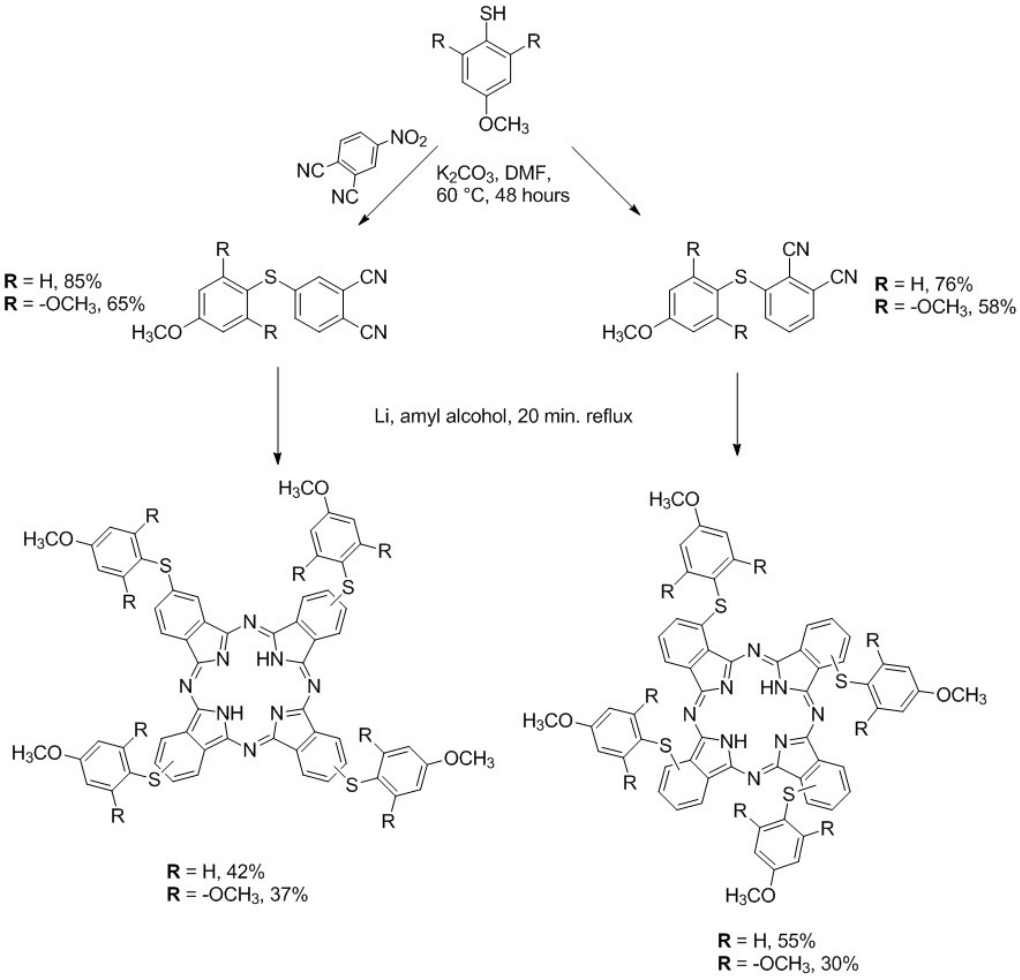

Scheme 2: Pre-functionalization of phthalocyanine with methoxyphenylthio- groups by Odabas et al.[38]

The pre-functionalization of phthalocyanines with naturally abundant monoterpenes has been carried out by sustainable synthetic approaches such as ultrasound and microwave irradiation by Pereira et al. The results did not differ significantly from conventional synthesis, but the reaction times were lowered. In their work, ultrasound was the best alternative method for the introduction of the terpenes in the phthalonitrile, whereas microwave irradiation produced the better outcome in the macrocyclization reaction. This showcases the possibility of introducing cheap naturally abundant precursors for the synthesis of phthalocyanines based on biomateri-

als.[40] Glycosylated phthalocyanines have also been synthesised by the introduction of the carbohydrate moiety to the phthalonitrile precursor by nucleophilic aromatic substitution using typical conditions.[41;42]

This synthetic strategy has also been utilized in the synthesis of unsymmetrical substituted zinc phthalocyanines for antimycotic activity studies by Cosimelli et al.[43] and it is also the usual manner to obtain octasubstituted phthalocyanines from disubstituted phthalonitriles.[44] Leznoff et al. has also investigated the preparation of multisubstituted phthalonitrile precursors for phthalocyanine synthesis by means of nucleophilic aromatic substitution from tetrafluoro- and tetrachloro- phthalonitriles.[45]

Post-functionalization approach

The post-functionalization approach, namely the modification of already existing phthalonitriles, remains a largely unexplored route responding to common practical challenges regarding their lack of solubility and tendency to aggregate. Successful modifications of tetrasubstituted phthalocyanines include esterification,[46] reduction of nitro group[26] and removal of protecting groups,[47] among others. Recently, copper (I)-catalysed azide-alkyne cycloaddition click reactions have found interesting applications in the functionalization of phthalocyanines through this approach.[48;49] The use of S_NAr in phthalocyanines is largely absent in literature with only few examples, perhaps in part due to the difficulty in controlling the range of substitution achieved. Sample and Senge in their review of nucleophilic aromatic substitution of porphyrinoids devotes a small section to its use in phthalocyanines with a handful of examples mostly revolving around the substitution on zinc hexadecafluorophthalocyanine specifically.[50]

In one example, Lin et al. performed S_NAr in both the precursor and the subsequent phthalocyanine generating a tetra-substituted octanethio- in the presence of sodium hydride (**Scheme 3**). In their method, a bi-substituted phthalonitrile precursor was prepared equipped with bromo- and nitro-substituents, after which it was tetramerized with a copper salt at 180 °C producing a phthalocyanine where the bromo- activated by an ortho- nitro group could be readily substituted by 1-octanethiol.[51]

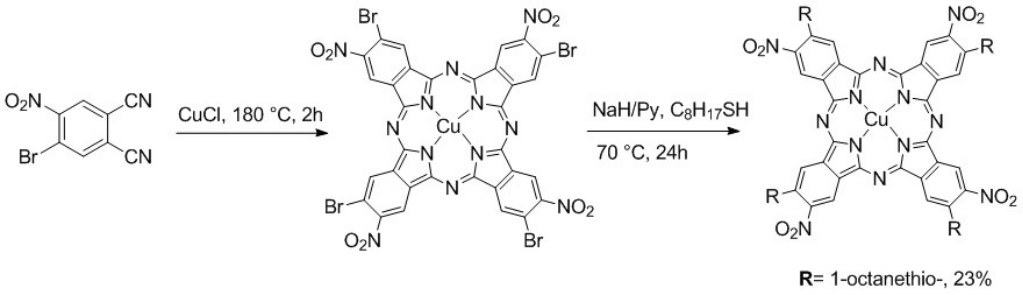

Scheme 3: Postfunctionalization of phthalocyanine by S_NAr done by Lin et al.[51]

Leznoff and co-workers have devoted much work to the study of multisubstituted phthalocyanines. In their first paper regarding post-functionalized phthalocyanines, Leznoff and Sosa-Sanchez investigated the nucleophilic substitution of hexadecafluorophthalocyaninato zinc(II) leading to a mixture of polysubstituted phthalocyanines characterized by matrix-assisted laser desorption/ionization (MALDI) analysis. Only two of the nucleophile candidates achieved full substitution probably due to less steric demand, although the yields were low.[52] The synthesis of polyaminosubstituted phthalocyanines was also investigated by Leznoff using different methodologies, unsurprisingly affording mixtures of aminophthalocyanines with varying degree of substitution. Interestingly, amine-linked phthalocyanines were formed from intramolecular nucleophilic substitution as indicated by mass spectrometry.[53]

The synthesis of glycosylated phthalocyanines from preliminary functionalized phthalocyanines has been reported by Drain and co-workers, affording a purely β-

substituted octathioglycosylated product from hexadecafluorophthalocyanine in the presence of potassium carbonate (K_2CO_3) (**Scheme 4**). This highlights the influence of the steric properties of the nucleophile on the substitution patterns and how the different reactivity of fluorine atoms on α- and β- position can be used to the chemist's advantage.[54] The review on synthetic approaches to glycophthalocyanines by Tome et al. contains several examples in the use of this method.[55]

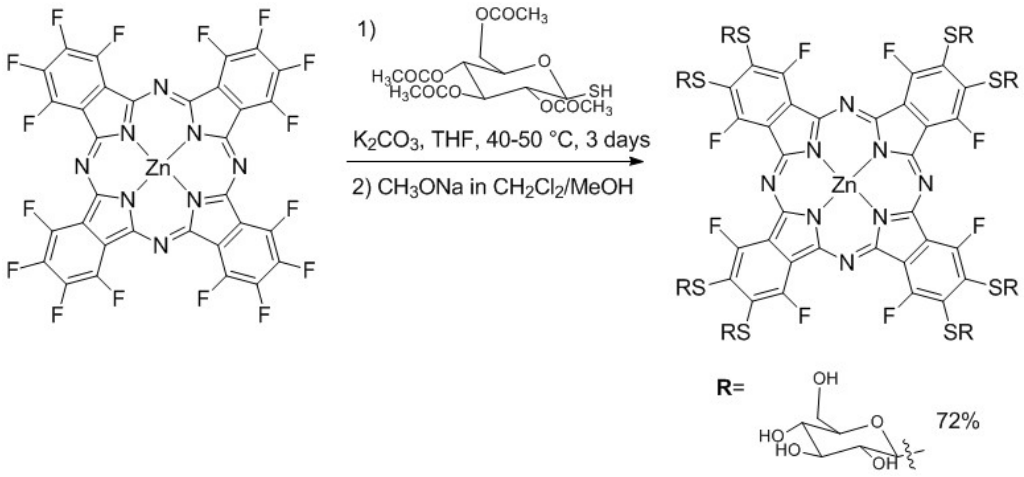

Scheme 4: Glycosylation of hexadecafluorophthalocyanine by Drain et al.[54]

The synthesis and functionalization of phthalocyanines by S_NAr has countless examples in literature that showcase its potential to create phthalocyanines with properties that can be tailored as desired. However, there is still lack of research on greener alternatives to their functionalization, in both the nucleophilic aromatic substitution of phthalonitriles pre-tetramerization and the functionalization of already tetramerized ones. In this light, our work pretends to investigate the use of nucleophilic aromatic substitution in the synthesis of phthalocyanines through a mechanochemical approach that provides a more sustainable manner for the synthesis of these organic dyes.

2.2 Mechanochemistry

Mechanochemistry focuses on driving chemical transformations by mechanical force through grinding, milling or compressing materials together manually or automatically by the use of milling or extrusion equipment (**Figure 2.3a**). The use of mechanical impact to modify matter has been observed since the early stages of human development.[56] The mortar and pestle for grinding have been in use since the Stone Age with many applications and while its intended use was particle size reduction, unintended chemical changes surely accompanied it. One of the first examples of mechanochemical reactions described in the annals of history is the reduction of cinnabar to mercury by grinding in a copper mortar (315 B.C).[57]

The first systematic studies of mechanochemical reactions started in the late 19th century and the development of the field was slow for most of the 20th century. The use of mechanochemical methods for chemical production has only recently emerged in response to environmental challenges that demand greener alternatives for sustainable chemical synthesis. As exemplified by the fifth principle of green chemistry that states: "The use of auxiliary substances (e.g., solvents, separation agents, etc.) should be made unnecessary wherever possible and, innocuous when used"[58] mechanochemistry becomes a feasible alternative for the elimination or at least significant reduction of organic solvents, many of which are volatile organic compounds (VOC's).

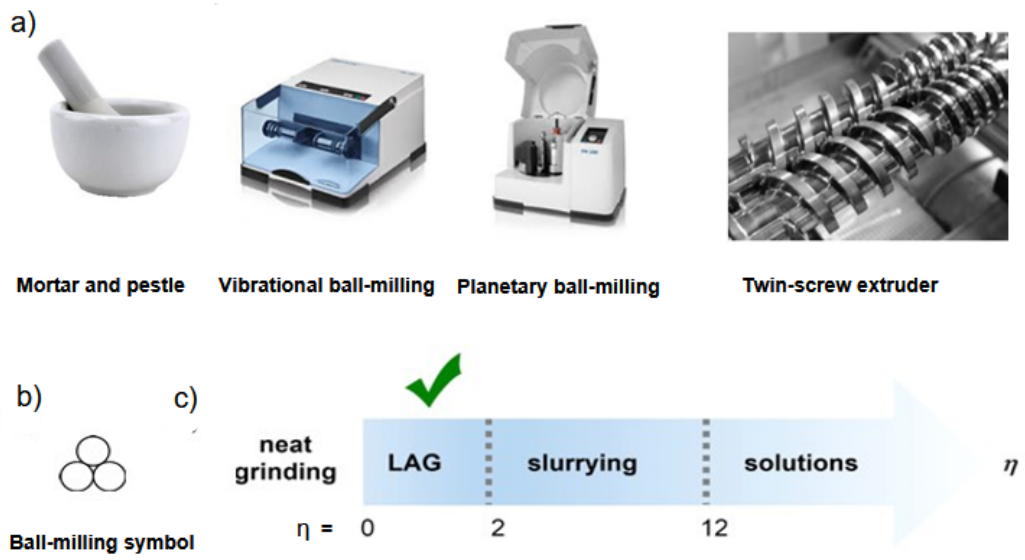

Figure 2.3: a) Common grinding and milling apparatus. b) Reaction symbol for ball-milling process. c) LAG scale.

In 2019 the IUPAC named mechanochemistry and reactive extrusion in their top ten of emerging technologies with the potential to make our planet more sustainable.[59] Significant advantages of mechanochemistry are the reduction of waste and reaction time, as well as resulting in improved yields, enhanced selectivity and good stoichiometric control. Current drawbacks arise from lack of fundamental knowledge in the energetics and thermodynamics of mechanochemical processes and poor understanding of the mechanisms in which most reactions occur.[60] Furthermore, the reproducibility of mechanochemical reactions can suffer from variations in the many factors involved that play an important role such as the mixing equipment (ball mill, planetary mill, etc), the milling speed, filling factor, ball properties and jar specifications, many of which often go unreported.[61]

Mechanochemical reactions can be conducted completely solvent-free or with the aid of a small amount of solvent. This approach to solid-state reactions is known as

liquid-assisted grinding (LAG) and it consists of the use of small amounts of liquid as an additive to enhance reactivity. The empirical characterization of LAG is done by the parameter η which accounts for the ratio of the liquid volume to the mass of the reactants and is expressed in µL/mg.[62] LAG is characterized as lying in the range of 0-2 µL/mg, whereas a typical solution reaction would have $\eta > 12$ µL/mg (**Figure 2.3c**). Some advantages offered by this approach are increased reaction rates, enhanced mass transfer and increased scope of potential reactants and products, among other.[58]

The use of mechanochemistry in organic synthesis has been well-documented[63;64;65] in recent years by the development of solid-state alternatives to common synthetic methods. Solvent-free syntheses are known for metal-catalyzed coupling reactions such as Suzuki,[66] Sonogashira[67] and Heck[68]. Solid-state condensation reactions such as aldol condensation,[69] Michael addition[70] and imine formation[71] have been extensively reported with high yields. It has also found interesting applications in click chemistry[72] and cascade reactions[73], as well as in different types of nucleophilic additions[74] such as Wittig reaction,[75] showcasing its broad applicability and versatility. The use of solid-state synthesis to drive nucleophilic aromatic substitution has been the subject of exploration in recent years and will be discussed in detail below.

2.3 Nucleophilic aromatic substitution

Nucleophilic aromatic substitution is a type of substitution reaction, in which the nucleophile (**Nu**) displaces a leaving group (**LG**), usually halogen or nitro-, in an electron-poor aromatic ring equipped with electron withdrawing groups (**EWG**) such as carbonyl, nitro or nitrile. There are various mechanisms in which this reaction can take place, the most common being the addition-elimination (S_NAr)[76]

(**Figure 2.4**).

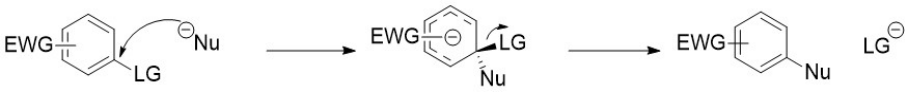

Figure 2.4: The basic mechanism of addition-elimination ($\mathbf{S_NAr}$) nucleophilic aromatic substitution.[76]

This reaction has played an important role in the synthesis of chemicals by exploiting the possibility of introducing functional groups on aromatic moieties with the replacing of a leaving group. Its effectiveness and simplicity have made it a staple in pharmaceutical and industrial chemistry. The reaction is an important synthetic tool in the functionalization and modification of porphyrinoids such as phthalocyanines. It is usually utilized to modify the phthalonitriles as desired before the macrocyclization into phthalocyanines[50], but the reaction allows for post-functionalization as well.

However, the reaction conditions for S_NAr can be harsh, often requiring high temperatures and long reaction times, coupled with the use of polar aprotic solvents. Specially problematic is the use of DMF, which has known reproductive and hepatic toxicity and has been the subject of strict European Union regulations recently.[77] This makes S_NAr a target for the development of greneer methodologies in its process.[78]

The use of the mechanochemical approach to drive nucleophilic aromatic substitution remains underdeveloped despite its versatility, although this has been changing in recent years. Recently, Andersen studied the kinetics of S_NAr reactions both in solution and in solid-state with temperature control, reporting a significant rate and yield enhancement with the mechanochemical approach.[7] In the benchmark exam-

ple, 1-chloro-4-nitrobenzene was reacted with piperidine in the presence of a base at 100 °C in both 1.0 M DMF solution and ball milling, resulting in an increased yield and nine times faster conversion (**Scheme 5**). A similar trend was observed, when the comparison was applied to other nucleophiles. In a follow-up study by Andersen, the influence of temperature on conversion was reported and different mechanochemical methods (ball milling and extrusion) were compared.[79]

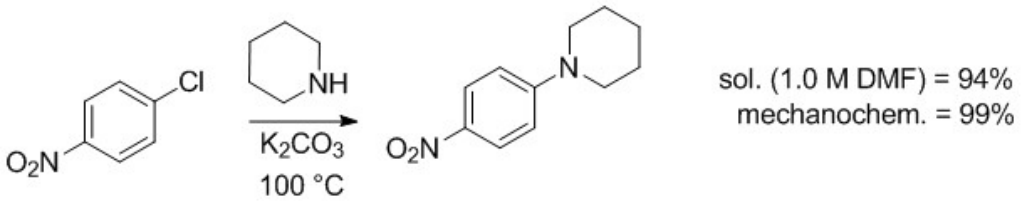

Scheme 5: Benchmark mechanochemical and conventional S_NAr reaction in Andersen's paper.[7]

Similarly, Vaghi et al. reported the mechanochemical nucleophilic aromatic substitution of fluoroaromatic compounds and piperidine using aluminum oxide as auxiliary, which afforded yields greater than 90% in many cases (**Scheme 6**).[78] The mechanochemical reaction harnessed the excellent affinity of Al_2O_3 for hydrogen fluoride, leading to increased conversions and affording many pharmaceutical precursors in high yields with simple and fast work-up.

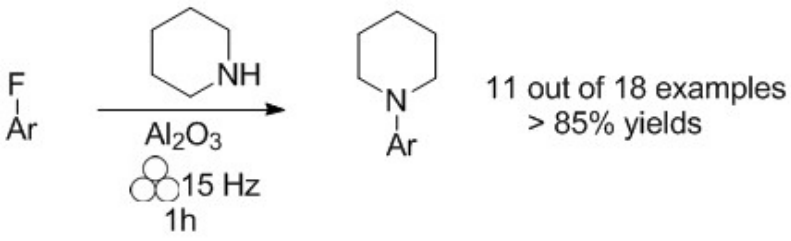

Scheme 6: Mechanochemical S_NAr of fluoroaromatic compounds by Vaghi et al.[78]

Mkrtchyan et al. developed a protocol for the conversion of aromatic amines to aryl trifluoromethyl ethers by ball milling in a one pot procedure with the aid of

pyrylium tetrafluoroborate reagent to activate the amines and a $-OCF_3$ source (**Scheme 7**). This allowed for the substitution of more than thirty anilines with optimal yields averaging 70-80%.[80] Inspired by the success of this protocol they also investigated the mechanochemical synthesis of trifluoromethyl arenes by nucleophilic aromatic substitution in a convenient one-pot procedure from aromatic amines supported by nanocellulose, reporting excellent yields (**Scheme 8**). This protocol offers a greener alternative to the production of pharmaceuticals and late-stage functionalization of active pharmaceutical ingredients.[81] In a follow-up paper, Mkrtchyan's group extended this approach to the formation of trifluoromethoxy moieties from aryltrimethylammonium triflates, aryldiazonium tetrafluoroborates and aryl pinacolboranes (**Scheme 9**).[82]

Scheme 7: Synthesis of aryl trifluoromethyl ethers from anilines by ball-milling.[80]

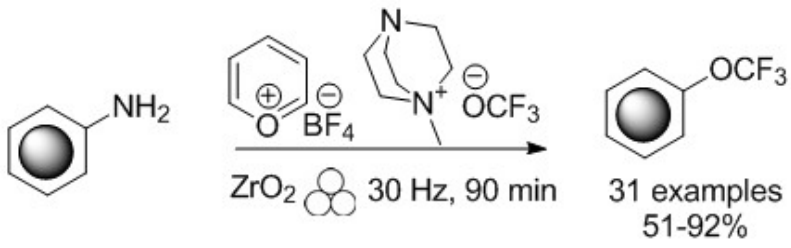

Scheme 8: One-pot mechanochemical synthesis of trifluoromethyl arenes by S_NAr.[81]

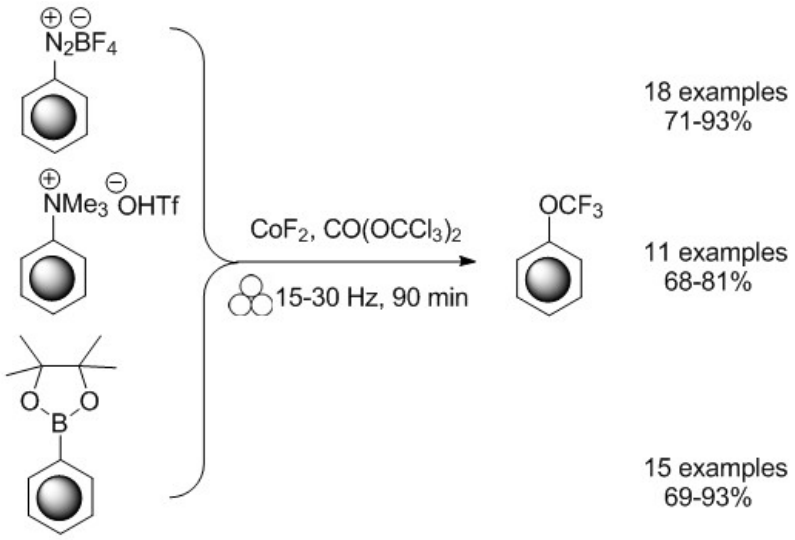

Scheme 9: Mechanocemical synthesis of trifluoromethoxy compounds from aryltrimethylammonium triflates, aryldiazonium tetrafluoroborates and aryl pinacolboranes.[82]

An environmentally friendly one-step hydroxylation of aryl fluorides by ball milling was reported by Rodrigo et al. Their approach consisted of a nucleophilic aromatic substitution of the fluoroaromatic compound with KOH as hydroxyl source and a crown ether additive in solvent-free conditions. With this method, aryl and heteroaryl hydroxyls were afforded in medium to excellent yields, providing a convenient approach without the use of any solvent or external heating.[83]

In a liquid-assisted grinding (LAG) approach to the nucleophilic aromatic substitution of fluorinated phthalonitriles with carbazole, Leitch et al. successfully synthesized carbazole-based isophthalonitrile fluorophores and related compounds (**Scheme 10**). In their optimization of reaction conditions they arrived at a 92% yield with the use of THF in 1 µL/mg liquid to solid ratio with 30 minutes of pre-milling the base and carbazole and 30 minutes of milling after the addition of the LAG agent and the fluorophthalonitrile. The scope of the project afforded the synthesis of a small library of phthalonitrile fluorophores with 60-90% yields after

column chromatography.[84]

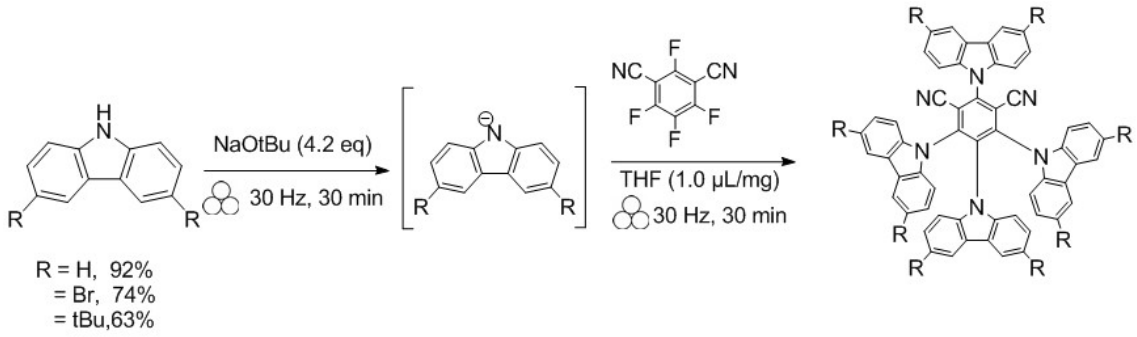

Scheme 10: LAG S_NAr of fluorophthalonitriles with carbazole by Leitch et al.[84]

These examples showcase the growing interest in moving nucleophilic aromatic substitution away from the heavy use of polar aprotic solvents such as DMF into alternatives that greatly reduce the need of solvent and intensive heating. Furthermore, besides decreasing the environmental impact, the versatility of this reaction could aid the green functionalization of a vast array of materials and pharmaceuticals and could prove effective for materials of problematic solubility.

3. Aims and objectives

The synthesis of functionalized phthalocyanines traditionally relies on large amounts of polar aprotic solvents and prolonged, heat-intensive reaction times, contributing significantly to the environmental footprint of the process. Although recent efforts have aimed to develop greener alternatives for phthalocyanine synthesis, the sustainable synthesis of functionalized phthalocyanines remains a challenge. Moreover, many of these methods fail to account for the inherently low solubility of phthalocyanines, which limits their practical applicability. In this context, the exploration of a mechanochemical approach to synthesizing functionalized phthalocyanines by S_NAr presents a compelling and environmentally conscious alternative aimed at reducing organic solvents and energy use.

In this study, we explore the feasibility of a mechanochemically driven S_NAr reaction for phthalonitrile derivatives, optimizing the conditions by systematically screening key parameters such as LAG volume, base equivalents, and milling time. We assess the impact of these variables on both the efficiency and reproducibility of the reaction, providing insight into the mechanistic and practical aspects of this solvent-minimized approach.

Additionally, we broaden the scope of the reaction by examining a diverse range of nucleophiles and phthalonitrile substrates, delving into the fundamental reactiv-

ity trends of mechanochemical S_NAr processes. The subsequent tetramerization of these intermediates into their corresponding phthalocyanines is also briefly investigated, laying the groundwork for future studies and paving the way toward the development of a streamlined one-pot synthesis.

4. Results and discussion

Inspired by the success of our group's previous investigation regarding the solid-state synthesis of phthalocyanines from phthalonitriles[27], we set out to direct our research towards the mechanochemical functionalization of the phthalonitriles by S_NAr. This way, we could create a sustainable synthesis of phthalocyanines in two steps with minimal solvent use, advancing closer to the one-pot ideal. Furthermore, the mechanochemical S_NAr of phthalonitriles has not been investigated.

4.1 Optimization

4.1.1 Preliminary optimization

For the preliminary studies on the feasibility of mechanochemical S_NAr and its optimization, 4-nitrophthalonitrile and 3-hydroxypyridine were chosen as our model substrate and nucleophile, respectively (**Figure 4.1a**). This choice responded to the cheap availability of the starting materials compared to similar nitrophthalonitriles and hydroxypyridines.

In our initial studies, we explored variations in both the solvent type, switching between DMF and dimethylsulfoxide (DMSO), and the LAG volume, adjusting between 50 µL (0.026 µL/mg) and 100 µL (0.052 µL/mg). The reactions were performed using 10 equivalents of K_2CO_3, with the nucleophile in a 1.3-fold excess,

and milled for 30 minutes at 25 Hz. After milling, the crude reaction mixture from the jar was analyzed by ^{1}HNMR by simply dissolving a sample in d_6-DMSO and filtering out the salt. The resulting spectra appeared clean (**Figure 4.1c before extraction**), leading us to mistakenly believe that full conversion had been achieved. However, thin-layer chromatography (TLC) results told a different story, particularly in the completely solvent-free reaction. Despite the ^{1}HNMR spectrum indicating complete conversion, TLC revealed minimal product formation relative to the starting material.

This prompted us to search for an extraction system that would yield accurate results. After evaluating acetone and ethyl acetate as potential extraction solvents, we chose the latter due to its better reproducibility and closer alignment with the TLC results. With this system in place, we began analyzing the extracted crude by ^{1}HNMR to determine accurate conversion rates (**Figure 4.1c after extraction**).

The solvent-free reaction resulted in very low conversions of the starting materials, and without a base, no reaction occurred (**Figure 4.1 d**). The choice between DMF and DMSO had little impact on the outcomes, leading us to select DMSO due to the stringent European Union regulations surrounding DMF. Additionally, varying the ratios of starting materials did not significantly affect the results, so we opted for a 1:1 ratio to minimize waste (**Figure 4.1 b**). The amount of K_2CO_3 was likewise reduced from 10 equivalents to 3 with no important changes.

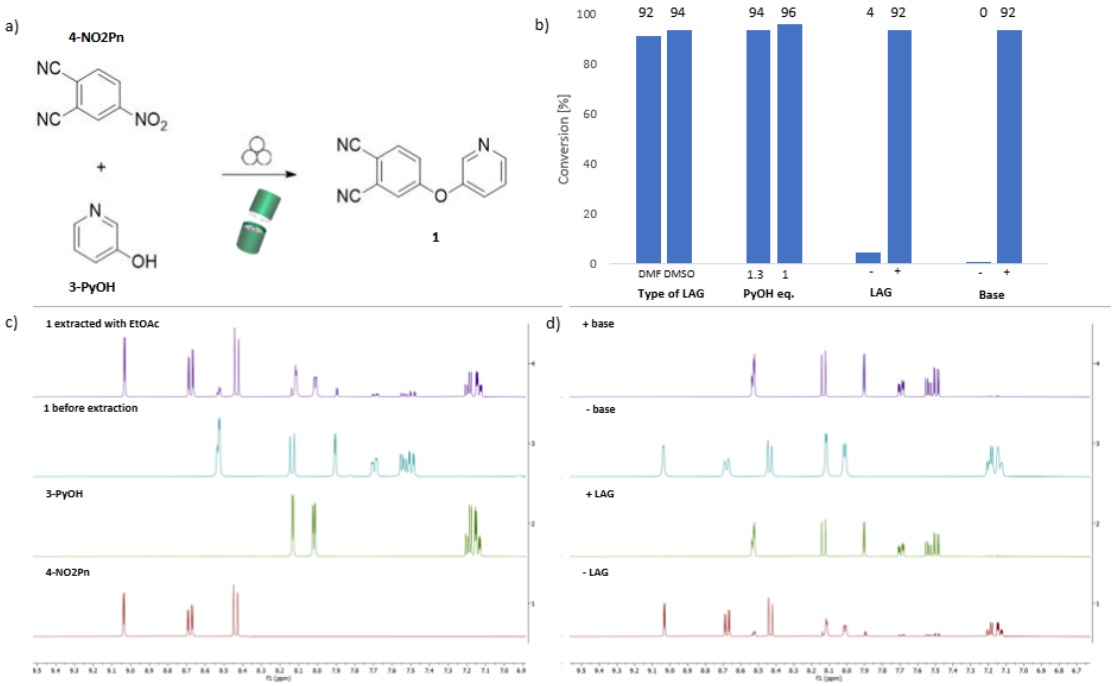

Figure 4.1: a) Benchmark reaction. b) Preliminary studies on the feasibility of mechanochemical S_NAr. c) Comparison of ^{1}HNMR spectra of starting materials and crude before extraction and after extraction with EtOAc for entry 1 in **Table 1** (solventless reaction). d) Influence of the use of LAG and base in the reaction. Only aromatic region shown for clarity.

While investigating the influence of liquid quantity, we determined that the lowest amount that maintained good results without compromising the conversion was 25 µL (0.031 µL/mg). This led us to attempt to evaluate the influence of milling time on the reaction using the optimized reaction conditions (1:1 ratio of **4-NO_2Pn** and **3-PyOH**, 3 eq.K_2CO_3, 25 µL DMSO (0.031 µL/mg).

Initially, we attempted to take small samples at different time intervals during the reaction. However, the results proved unreliable due to homogenization issues, as sampling altered the mixture's properties, affecting its consistency and accuracy. This led us to conduct milling experiments with varying durations, extracting full

Table 4.1: Optimization studies of benchmark reaction

Entry	V DMSO (µL)	Eq. K_2CO_3	Time (min)	η (µL/mg)	Average Conv. (%)
1	**0**	3	30	0	4 ± 0
2	**10**	3	45	0.013	28 ± 8.
3	**25**	**3**	**45**	**0.031**	**96 ± 3**
4	**50**	3	45	0.063	92 ± 5
5	25	**1.5**	45	0.045	9 ± 9
6	25	**10**	45	0.013	51 ± 9
7	25	3	**15**	0.031	74 ± 26
8*	25	3	**30**	0.031	43 ± 51
9	25	3	**30**	0.031	81 ± 10

* without pretreatment in vacuum oven. In bold: optimized conditions

batches for analysis. We found that the reaction could reach very high conversion rates in just 15 minutes, but reproducibility was poor. Even at our 30-minute benchmark, conversion remained high but with significant outliers. This issue became more pronounced as ambient moisture increased, severely hindering the reaction. To address this, we extended the milling time to 45 minutes and pre-treated the starting materials in a vacuum oven before the reaction, which resulted in improved consistency and reliability.

After establishing these optimized conditions, we investigated the influence of several variables on the reaction, focusing primarily on LAG amount, K_2CO_3 equivalents, and milling time, as these proved to have the most significant impact (**Table 4.1**).

4.1.2 Volume of LAG agent

Our LAG agent of choice was DMSO, an aprotic polar solvent ideal for S_NAr reactions and less toxic than the commonly used DMF. The purpose of the LAG is to create homogenization through a mobile phase that brings the reactants in close contact, enabling the reaction. In our study, while the solventless reaction did yield some minor product formation, LAG proved essential for achieving higher conversion rates from starting materials to the desired product.

Having confirmed the importance of LAG, we investigated different liquid-to-solid ratios by varying the solvent amount while keeping the total mass of reactants constant, conducting experiments in triplicate . The results demonstrated that the reaction could proceed efficiently with an η as low as 0.031 µL/mg, which is an order of magnitude below the upper limit typically considered for LAG. This notable result showcases the adaptability of S_NAr to minimal solvent and room temperature conditions (**Figure 4.2**).

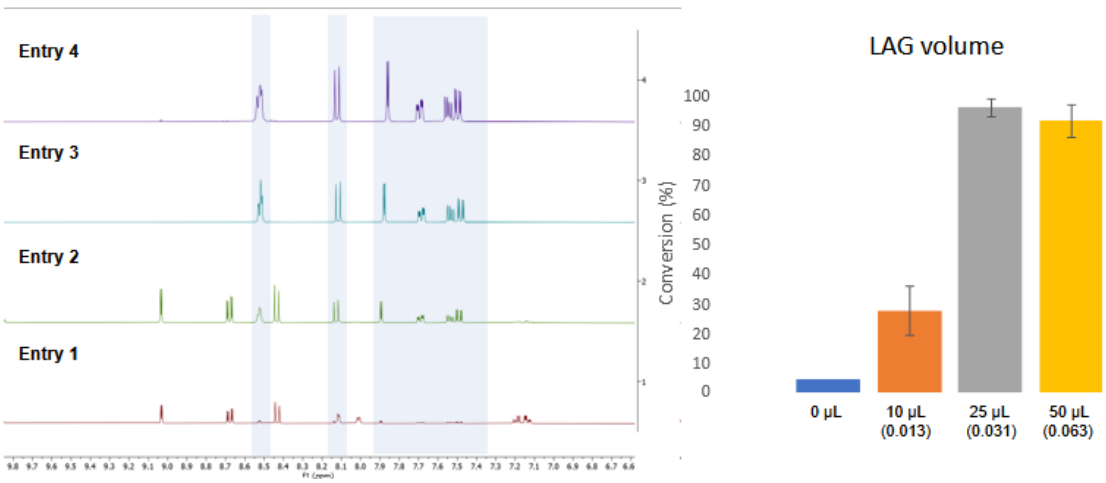

Figure 4.2: Influence of LAG volume in the benchmark reaction from **Table 4.1**.Highlighted in blue, the peaks corresponding to product **1**

4.1.3 Equivalents of base

The reaction fails to proceed without a base capable of deprotonating the nucleophile before it can attack the phthalonitrile. Potassium carbonate is the preferred base for S_NAr reactions, and its bulky solid nature makes it particularly well-suited for ball milling. The use of triethylamine as a base and LAG agent simultaneously was briefly attempted, yielding no results.

Since the number of potassium carbonate equivalents can influence reactivity by altering the liquid-to-solid ratio, we decided to investigate its effect on our benchmark reaction testing the use of 1.5, 3, and 10 equivalents. We found that reducing the potassium carbonate amount below 3 equivalents, despite increasing the liquid-to-solid ratio, was detrimental to the reaction, leading to consistently low conversions and poor reproducibility. This can likely be attributed to an insufficient number of deprotonated nucleophiles available for reaction, as well as a decrease in the jar's filling factor, which may cause material to stick to the walls, hindering reactivity. Conversely, increasing the base to 10 equivalents yielded better results, with one outlier achieving over 90% conversion. However, in general, reproducibility declined due to the reduced liquid-to-solid ratio, which may have impaired effective contact between reactants. Thus, using 3 equivalents of base provided the optimal balance, ensuring sufficient deprotonation while maintaining a liquid-to-solid ratio high enough to facilitate efficient reaction progress (**Figure 4.3**)

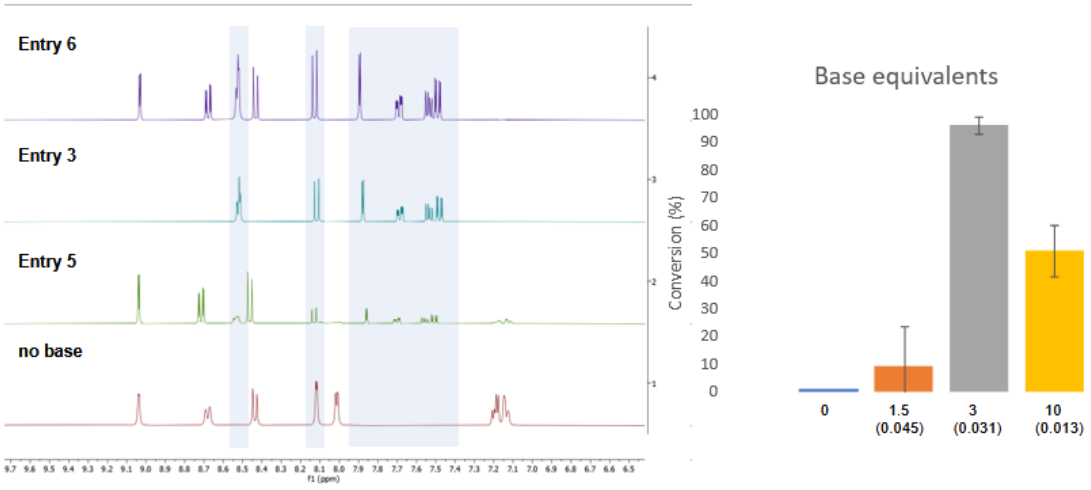

Figure 4.3: Influence of K_2CO_3 equivalents in the benchmark reaction from **Table 4.1**. Highlighted in blue, the peaks corresponding to product **1**

4.1.4 Milling times

The milling time plays a crucial role, not necessarily in determining the success of the reaction, but in ensuring its reproducibility and consistency. This was evident in our preliminary experiments, where the standard 30-minute milling time sometimes yielded conversions above 95%, while in other instances, conversions were significantly lower. To address this variability, we began pre-treating the starting materials, which helped improve consistency to some extent (see entry 8 and 9, **Table 4.1**).

With the optimized conditions in place, we evaluated the reaction's behavior at milling times of 15, 30, and 45 minutes (**Figure 4.4**). The results revealed a clear trend: while the reaction could reach near-full conversion in just 15 minutes, reproducibility was extremely poor, as indicated by the high standard deviation across triplicates. Extending milling to 30 minutes improved consistency, though conversions still varied widely between 65% and 95%. At 45 minutes, conversion remained consistently high, with an acceptable standard deviation, demonstrating that extended milling improved reliability.

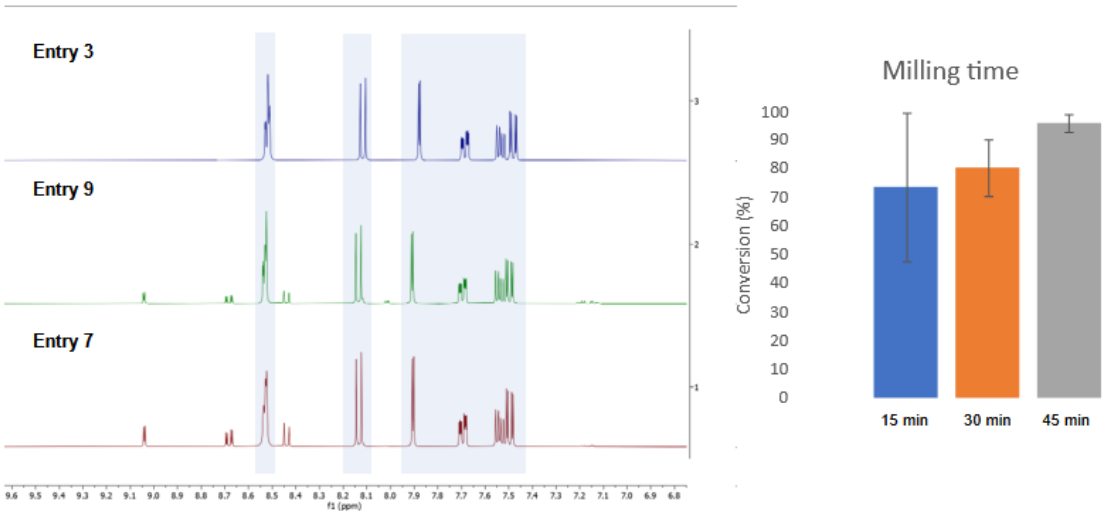

Figure 4.4: Influence of milling time in the benchmark reaction from **Table 4.1**. Highlighted in blue, the peaks corresponding to product **1**

The optimization studies underscored the critical role of LAG, base selection, and milling time in the mechanochemical S_NAr reaction. Under optimized conditions, the reaction proceeded nearly to completion (96 ± 3% conversion, 90% yield) with η = 0.031 µL/mg, 3 equivalents of base, and 45 minutes of milling, following pre-treatment of the starting materials in a vacuum oven. A 1:1 ratio of starting materials was maintained, and DMSO was identified as the preferred LAG agent.

4.2 Scope of nucleophiles

With the optimized conditions established, we sought to evaluate the robustness of the reaction by expanding the scope to selected nucleophiles. We chose five nucleophiles of particular relevance. The first two, 4-hydroxypyridine and 2-hydroxypyridine, were selected to assess how structural isomers of our benchmark nucleophile would react under the same conditions. Additionally, two sterically hindered phenols were included to examine the impact of steric hindrance on the reaction. Finally, we

selected a nucleophile from a different class to explore the potential extension of the reaction scope beyond phenols (**Figure 4.5**).

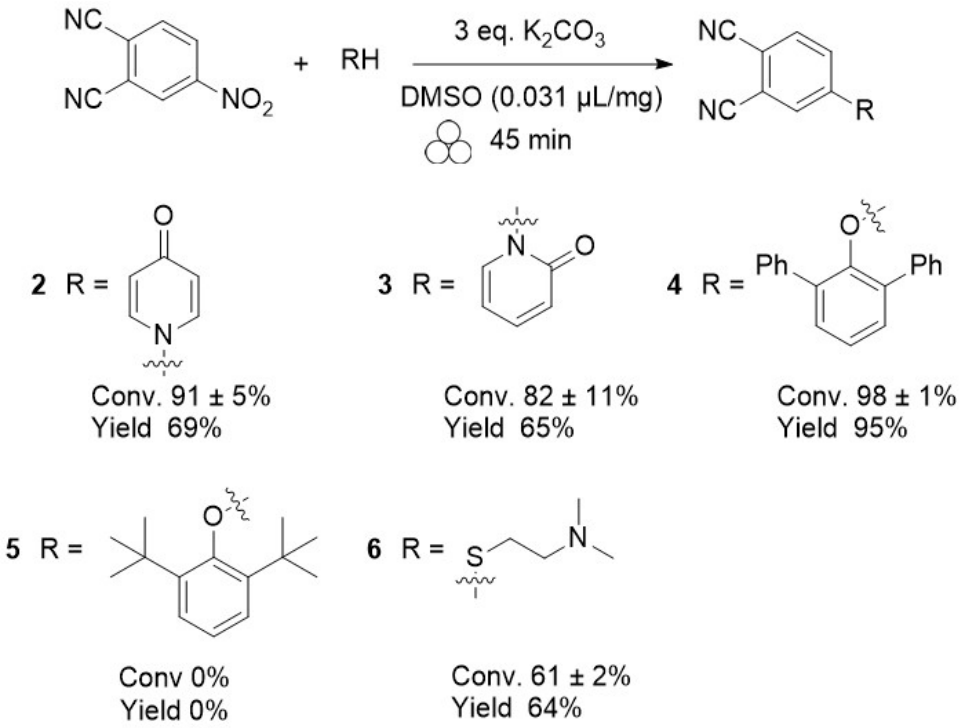

Figure 4.5: Scope of functionalization of 4-nitrophthalonitrile by S_NAr with different nucleophiles.

Unlike 3-hydroxypyridine, its structural isomers 4-hydroxypyridine and 2-hydroxypyridine exhibit keto-enol tautomerism, allowing the reaction to proceed through two possible pathways, either via deprotonation of the hydroxyl group or the amine from its tautomer (**Figure 4.6**). Surprisingly, in both cases, the reaction was found to proceed through the keto tautomer preferably, yielding oxopyridin derivatives rather than the pyridyloxy product observed in the benchmark reaction based on unusually high carbon shifts in ^{13}CNMR and IR bands in the 1600-1700 cm^{-1} range (see Appendix). This unexpected outcome suggests that the keto form is favored in the mobile phase created by LAG, though further investigation is needed to fully understand this behavior.

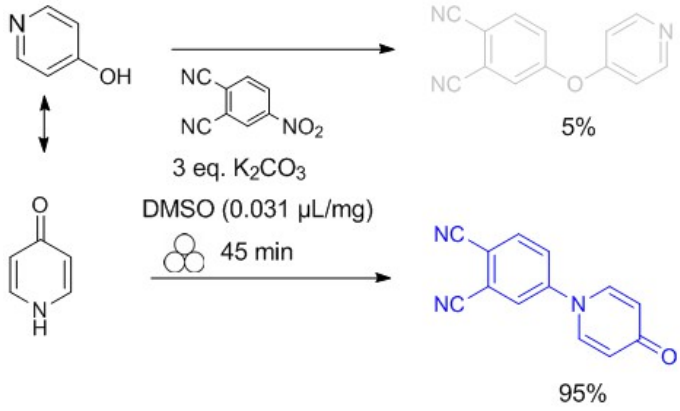

Figure 4.6: Reaction of 4-hydroxypyridine with 4-nitrophthalonitrile, exhibiting keto and enol reactivity.

The reaction between 4-hydroxypyridine and 4-nitrophthalonitrile yielded the oxopyridin **2** with an average conversion rate of 91% and a 69% yield across triplicates. The pyridyloxy forming from the enol tautomer was present in a 5% average. In contrast, the reaction with 2-hydroxypyridine exhibited lower conversion and yield, along with reduced reproducibility. The presence of the side product was only found in trace amounts.

The sterically hindered phenols investigated were 2,6-diphenylphenol and 2,6-di*tert*-butylphenol, both featuring bulky ortho-substituents adjacent to the hydroxyl group. For the diphenylphenol, the reaction typically reached near-full conversion to **4** and high yields under the benchmark conditions.

However, no product formation was observed for the di-*tert*butylphenol derivative by ^{1}HNMR, and the low-melting nature of the compound caused it to liquefy during milling. This suggests that the steric bulk of the *tert*-butyl groups hindered both deprotonation and nucleophilic attack, preventing the reaction from proceeding.

Lastly, 2-(dimethylaminoethane)thiol hydrochloride was reacted with our model substrate to form the corresponding thiophthalonitrile **6**. The reaction afforded moderate conversion and yield, just above 60%, but demonstrated excellent consistency across triplicates. This indicates that the reaction is feasible with thiol derivatives, though some adjustments to the benchmark conditions may be necessary to optimize performance.

Overall, the use of various nucleophiles in the mechanochemical S_NAr reaction highlighted the versatility of this methodology. However, minor optimization may be required on a case-by-case basis, as we will explore in the next section.

4.3 Scope of phthalonitrile substrates

We also aimed to expand the reaction scope by exploring various phthalonitrile substrates of interest, including a different nitrophthalonitrile isomer, as well as di- and tetra-substituted phthalonitriles with our benchmark nucleophile. Additionally, we took a brief detour to investigate the reactivity of different monosubstituted phthalonitriles in the mechanochemical S_NAr reaction (**Figure 4.7**).

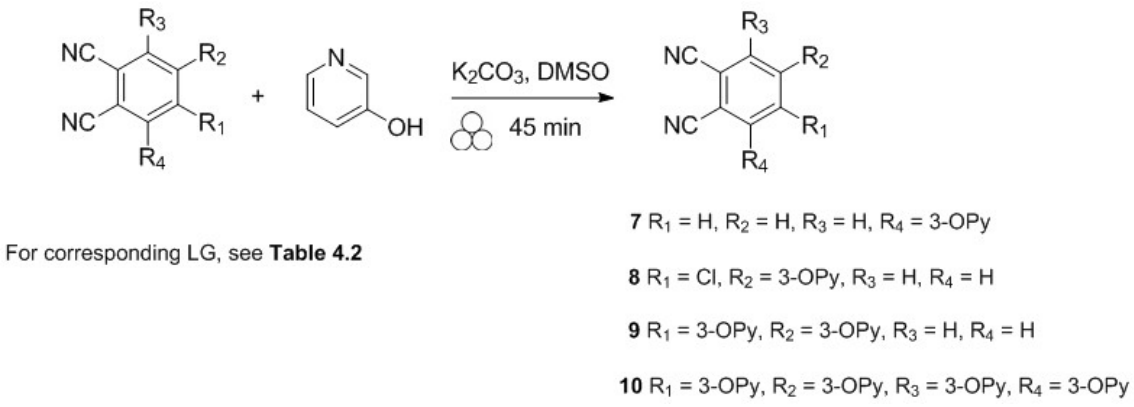

Figure 4.7: Scope of phthalonitrile substrates and leaving groups.

Table 4.2: Scope of mechanochemical S_NAr of different phthalonitrile substrates

LG	Prod.	η (µL/mg)	Conversion (%)	Yield (%)
$R_4 = NO_2$	**7**	0.031	97 ± 3	85
R_1= Cl, R_2 = Cl	**8**	0.77	97	96
R_2 = I	**1**	0.041	0	0
R_2 = Br	**1**	0.19	0	0
R_2 = Cl	**1**	0.16	0	0
R_2 = F	**1**	0.21	99	82
R_1 = F, R_2 = F	**9**	0.15	-	42
R_1 = F, R_2 = F R_3 =F, R_4 = F	**10**	0.20	-	56

To investigate the influence of nitro-group positioning on reactivity, we selected 3-nitrophthalonitrile as a substrate. Using the optimized conditions from the benchmark reaction, we achieved an average conversion rate of 97% across triplicates with an 85% yield of **7**. This demonstrated that the reaction proceeded nearly to full conversion, regardless of the nitro-group's position on the phthalonitrile core.

Next, we attempted to synthesize a disubstituted bispyridyloxy phthalonitrile using 4,5-dichlorophthalonitrile as the electrophile. However, under our optimized conditions, the reaction achieved only 20% conversion, with substitution occurring at only one of the chloro positions. To improve reactivity, we increased the nucleophile equivalents to 4 and raised η to 0.77 µL/mg, representing a 20-fold increase from our benchmark conditions while still remaining within the LAG range. This adjustment significantly improved conversion to 97%; however, only one chloro- leaving group was substituted, yielding product **8** (**Figure 4.8**). We hypothesize that the failure to obtain the fully disubstituted product may be due to the electron-donating nature of the pyridyloxy group, which reduces the electrophilicity of the remaining

chloro-substituted position.

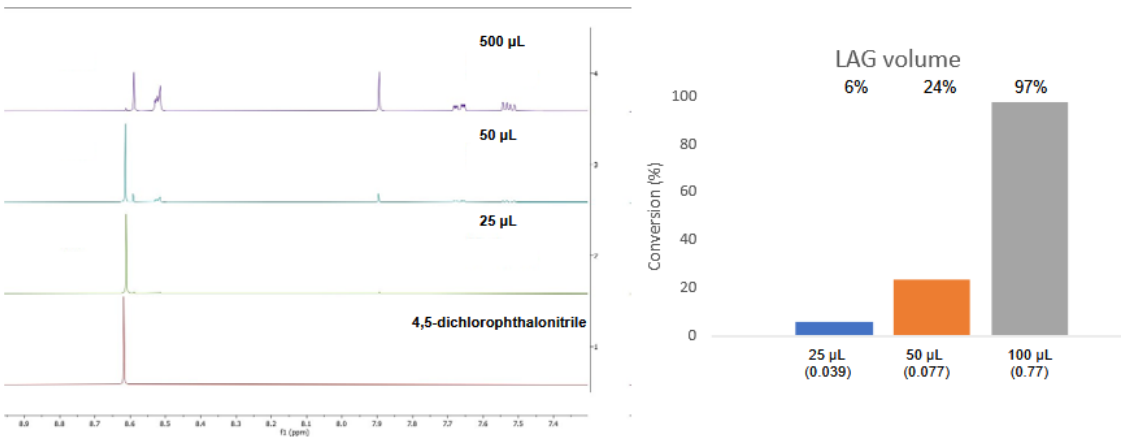

Figure 4.8: Influence of LAG volume in the conversion of 4,5-dichlorophthalonitrile to **8**

This intriguing result led us to investigate the reactivity of different leaving groups beyond the nitro group. We focused on 4-substituted phthalonitriles, specifically exploring halogen leaving groups, which are commonly used in S_NAr reactions (**Table 4.2**). To our surprise, the only halide that exhibited any reactivity under mechanochemical conditions was 4-fluorophthalonitrile. Neither 4-iodo, 4-bromo, nor 4-chlorophthalonitrile reacted with 3-hydroxypyridine, yielding only unreacted starting material, even when η was increased for the bromo- and chloro-substituted substrates. Notably, while 4,5-dichlorophthalonitrile allowed for a single substitution, the mono-chloro derivative remained entirely unreactive. Even 4-fluorophthalonitrile required optimization, with an increase in η to 0.21 µL/mg necessary to achieve full conversion.

After confirming that the fluoro leaving group could be substituted, we explored multisubstitution using 4,5-difluoro- and tetrafluorophthalonitriles under increased η conditions. For 4,5-difluorophthalonitrile, the reaction proceeded successfully at η

= 0.154 µL/mg, yielding a mixture of mono- and di-pyridyloxy products in approximately a 1:1 ratio. Following separation by column chromatography, the disubstituted pyridyloxy product **9** was obtained with a 41% yield. This was confirmed by ^{19}FNMR spectrum by the absence of fluoro signals. For tetrafluorophthalonitrile, the reaction proceeded efficiently at η = 0.200 µL/mg, yielding the tetrapyridyloxy phthalonitrile **10**. After column separation, the product was obtained in a 56% yield, demonstrating the feasibility of achieving multisubstitution using this mechanochemical approach.

Overall, the reaction exhibits a more limited scope with different electrophiles and allows for little variability in leaving groups, which is a common limitation in S_NAr reactions. Additionally, the reactivity of different leaving groups appears to be highly sensitive to changes in LAG conditions, often requiring further optimization to achieve successful substitution.

4.4 Primer on phthalocyanine formation

Although not the primary focus of this study, we sought to briefly explore the feasibility of synthesizing functionalized phthalocyanines from the prepared phthalonitriles. We applied the methodology previously developed by our group without further optimization. This approach utilizes a combination of milling and aging, where milling ensures thorough homogenization of the mixture, and aging at 120 °C for 48 hours facilitates the formation of phthalocyanines with minimal use of DMAE as both LAG and nucleophile.

We chose to synthesize zinc phthalocyanines from five functionalized phthalonitriles, with the primary goal of observing dye formation (**Figure 4.9**). In each case, the reaction mixture rapidly turned deep blue or green, indicating successful phthalo-

cyanine formation within minutes. After washing with water, the crude products were analyzed using standard characterization methods.

However, due to the strong tendency of phthalocyanines to aggregate in solution, NMR analysis was hindered by significant peak broadening, preventing proper characterization.[31] While the appearance of multiple new aromatic peaks suggested successful dye formation, distinguishing these signals from those of the aromatic starting materials was challenging, so conversions are not provided here. Purification is necessary for a more definitive characterization, but the limited solubility of phthalocyanines in most organic solvents complicates separation. Identifying suitable solvent systems for column chromatography will be an important next step in refining this process.

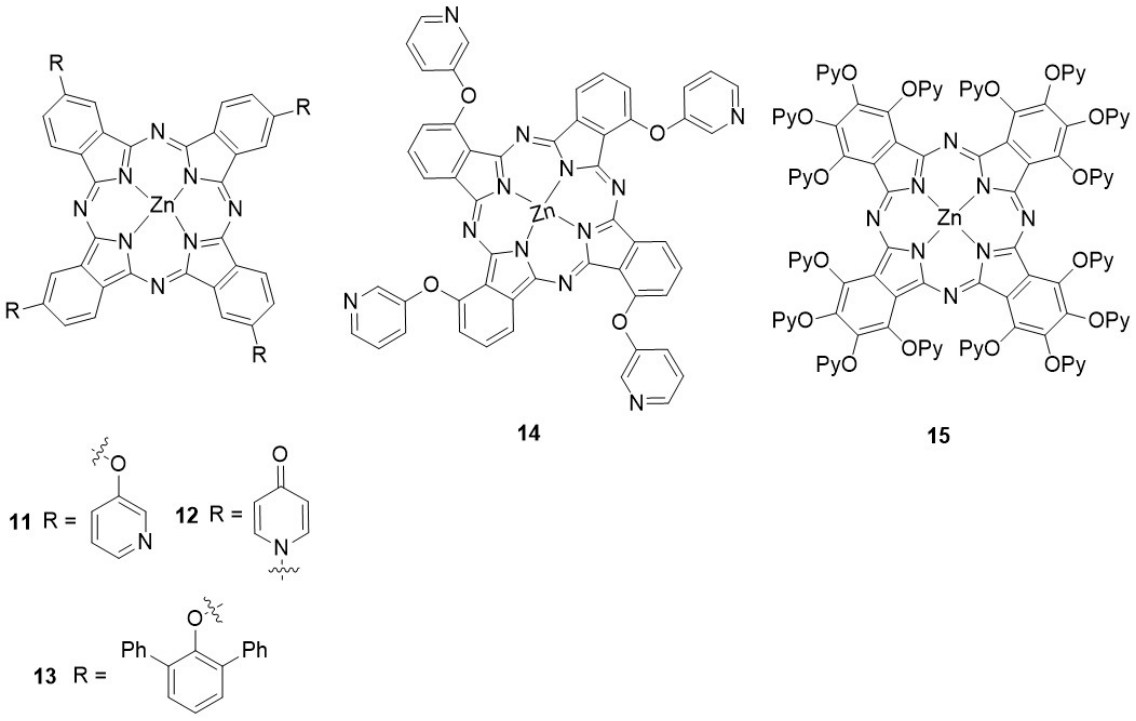

Figure 4.9: Synthesised phthalocyanines from previously prepared precursors.

Using MALDI-TOF analysis, we successfully confirmed the identity of four ph-

thalocyanines, demonstrating the feasibility of this synthetic route. However, an effective purification method still needs to be developed. Phthalocyanine **13**, which was soluble in THF, was analyzed by electrospray ionization (ESI) but could not be conclusively identified, likely due to decomposition during the measurement process.

Table 4.3: MALDI results from synthesised phthalocyanines

Pc	**From**	**DMAE (η = µL/mg)**	**Exact mass**	**Found in MALDI**
11	**1**	0.177	950.26	950.29
12	**2**	0.166	950.26	950.40
13	**4**	0.198	1554.45	N/A
14	**7**	0.153	950.26	950.30
15	**10**	0.194	2067.28	2068.38

These results lay a solid foundation for extending the research into the final tetramerization step; however, improved characterization methods will be essential for accurate assessment of the products. Additionally, a preliminary exploration of a post-functionalization approach using a nitro-substituted phthalocyanine was conducted toward the end of this study, but the outcomes were unsatisfactory, indicating that further optimization is required.

5. Conclusions and outlook

The synthesis of functionalized phthalocyanine precursors via mechanochemical S_NAr on phthalonitriles offers a promising route to access these pigments with significantly reduced environmental impact. In this work, we successfully achieved high conversions under remarkably low liquid-to-solid ratios, as low as 0.03 µL/mg, a notable accomplishment that underscores the efficiency and sustainability of the method.

To compare with conventional methods, we decided to survey three papers that offer a synthesis of phthalonitrile **1** through conventional means.[85;86;87] In each case, the solvent reduction was evident, ranging from 97 to 99 percent (**Figure 5.1**). Furthermore, the reaction time was lowered in every case, highlighting the efficiency that could be achieved by our approach.

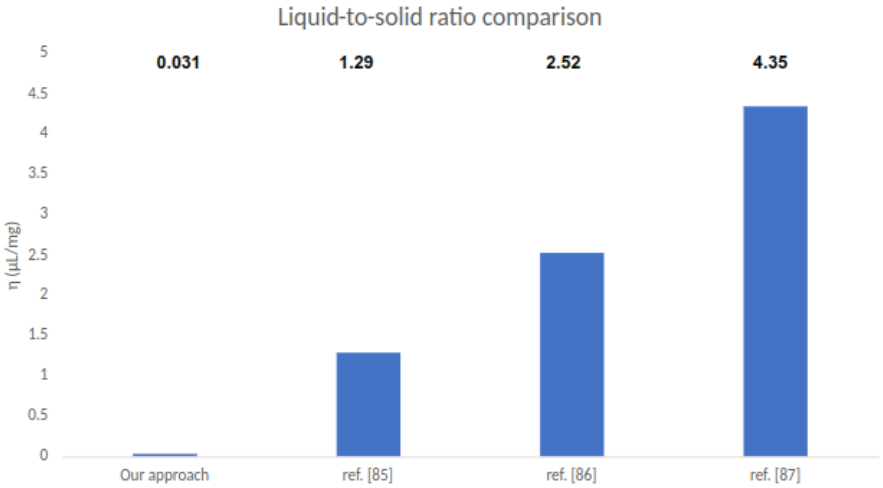

Figure 5.1: Comparing the solvent use of our approach with conventional proce-

dures.

The main limitations of our methodology stand on the necessity for optimization in a near case-by-case basis. We project this could be overcome by finding the liquid-to-solid threshold by which all reactions could proceed to >90% conversions, since this variable seems to be the most important one in the process.

The research could benefit from adding another dimension to the study by performing temperature-controlled experiments. We hypothesize that increasing the temperature could greatly aid the completion of the reaction aiming at reducing reaction times, based on previous examples[7]. Another necessary step forward is to investigate the performance of the reaction at large scale, moving towards extrusion systems commonly used in industrial settings. This could take our approach into a more streamlined procedure.

With relation to the phthalocyanines, isolation methods are to be developed and full characterization must be performed. Since we have seen that the reaction is feasible in the solid state with pre-milling, optimization might be necessary. Furthermore, the development of a one-pot system for the functionalization of phthalocyanines consisting on mechanochemical S_NAr followed by solid-state tetramerization might be a possibility, although the control of many variables needs more research. The mechanochemical post-functionalization approach could also be explored as an alternative, although the preliminary studies were not encouraging.

Overall, this work presents a comprehensive investigation into the mechanochemical S_NAr reaction of phthalocyanine precursors, systematically examining the influence of key variables under various reaction conditions. The versatility of the approach

is demonstrated through its application to diverse classes of nucleophiles and phthalonitrile substrates. Its potential for the sustainable production of functionalized phthalocyanines is also briefly explored. Finally, a balanced evaluation is provided, highlighting both the strengths and limitations of the methodology in comparison to conventional solution-based procedures, as well as the further outlook for the work in a broader scale.

6. Experimental section

6.1 Materials and methods

All chemicals were bought from commercial suppliers and used without further purification. Anhydrous DMSO was purged with argon before use. The pre-treatment of the reactants was done under vacuum oven in a Salvis KVTS 11 oven at 40 degrees for 1 hour, unless otherwise stated. The K_2CO_3 was kept at 120 °C in the oven before use

The ball milling was carried out in a Retsch MM400 mill in a stainless steel jar (14 mL) or zirconium jar (10 mL) with a single stainless-steel ball (4.0 g) or zirconium ball (3.0 g). All solid compounds were weighed on an analytical scale. The liquids used for this reaction were pippeted via Eppendorf Research Plus pipettes. The aging experiments were performed in a Salvis oven

The crude products from extraction were directly analysed without further purification, unless specified. The crude product was dissolved in d_6-DMSO and analysed by ^{1}HNMR. The devices used for performing NMR measurements were Bruker NMR Spectrometer AV III 400 and Bruker NMR Spectrometer AV NEO 400 operating at 400 MHz (^{1}H: 400 MHz, ^{13}C: 101 MHz). The probe temperature was kept at 23 °C unless otherwise stated The chemical shifts are given in ppm and calibrated

with the solvent signal given at 2.50 ppm (d_6-DMSO). Products were characterized when possible by ^{1}H, ^{13}C, COSY and HSQC. Mass spectrum of phthalonitriles was recorded with a Thermo Scientific ISQ EC with ESI (electrospray ionization). Mass spectrum from phthalocyanines was recorded by MALDI-TOF

6.1.1 Conversion rate calculation

The conversion rate was calculated from the average value of the integrals of the peaks belonging to the product and the starting materials. Peaks that showed overlap between starting materials and product, such as peak **b,k** from **Figure 6.1** were not considered in the calculations. The conversion was calculated using the following equation

$$\%(\mathbf{1}) = \frac{\bar{I}_{\mathbf{1}}}{\bar{I}_{\mathbf{1}} + \bar{I}_{4-PnNO_2} + \bar{I}_{3-PyOH}} \times 100$$

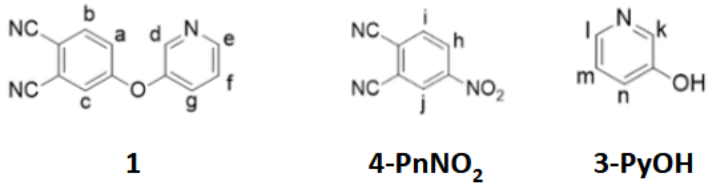

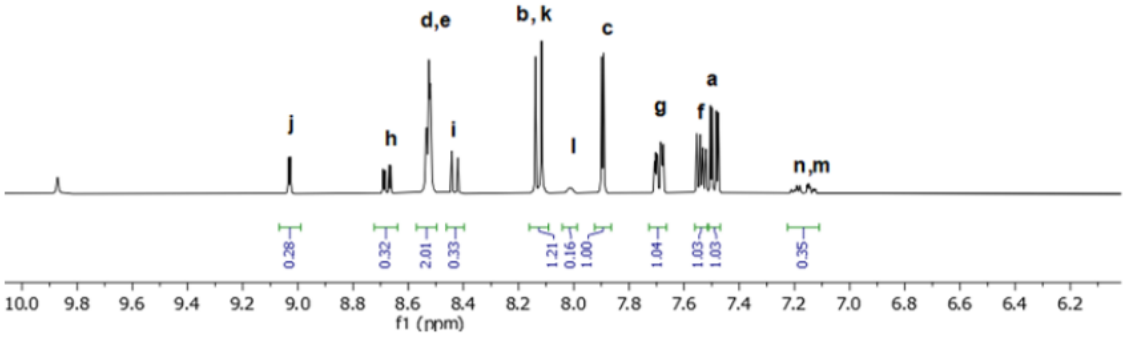

Figure 6.1:^{1}HNMR spectrum showing the peaks of product **1** and starting materials with the integrals used for conversions. Only aromatic region is shown for clarity.

The example in **Figure 6.1** would be calculated as follows

$$\begin{aligned}\%(\mathbf{1}) &= \frac{\frac{2.01+1.00+1.04+1.03+1.03}{6}}{\frac{2.01+1.00+1.04+1.03+1.03}{6} + \frac{0.26+0.32+0.33}{3} + \frac{0.16+0.35}{3}} \times 100 \\ &= \frac{1.018}{1.018 + 0.303 + 0.17} \times 100 \\ &= 68\%\end{aligned}$$

6.2 Experimental procedures

General procedure for the S_NAr of phthalonitriles

The phthalonitrile (1 eq) and the nucleophile (1 eq) were typically placed in a small vial and kept in the vacuum oven at 40 °C for 1 hour, unless otherwise stated. The solid mixture was added to a stainless steel milling jar containing a single stainless steel ball with anhydrous K_2CO_3 (3-10 eq.) and dry DMSO (0 - 0.2 µL/mg). The mixture was milled for 45 minutes at 25 Hz. The full batch was dissolved in 50 mL of water and 50 mL of ethyl acetate or dichloromethane (DCM), after which it was extracted 3 x 50 ml. The combined organic layers were washed with 100 ml brine, dried over anhydrous $MgSO_4$ and evaporated by rotary evaporator, yielding a crude solid that was analysed without further purification.

4-(pyridin-3-yloxy)phthalonitrile (1)

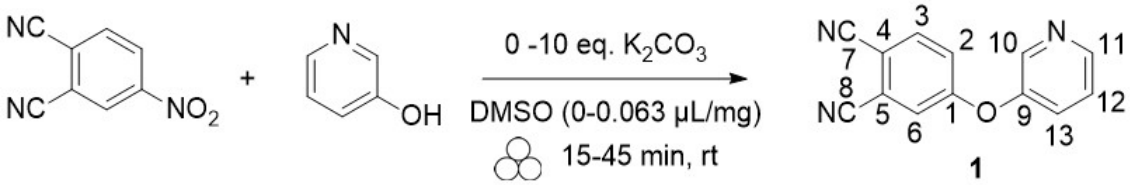

Synthesized from 4-nitrophthalonitrile (200 mg, 1.16 mmol) and 3-hydroxypyridine (110 mg, 1.16 mmol) in the presence of 1.5-10 eq. K_2CO_3 and DMSO (0-0.063 µL/mg) for 15-45 minutes according to the general procedure for S_NAr of phthalonitriles affording the crude as a brown solid (conversions on table).

^{1}H NMR (400 MHz, d6-DMSO) δ = 8.52 (2H, s, H-10-11), 8.13 (1H, d, H-3), 7.89 (1H, d, H-6), 7.68 (1H, m, H-13), 7.53 (1H, dd, H-12) 7.48 (1H, dd, H-2) ppm. (**Figure A1**)

^{13}C NMR (101 MHz, d_6-DMSO) δ = 160.5 (C-1), 150.8 (C-9), 146.8 (C-10), 142.2 (C-11), 136.4 (C-3), 128.0 (C-13), 125.2 (C-12), 123.0 (C-6), 122.5 (C-2), 116.9 (C-7), 115.8 (C-8), 115.3 (C-5), 108.9 (C-4) ppm. (**Figure A2**)

ESI-MS: m/z calculated for $C_{13}H_7N_3O$: 221.1; found 222.1 [M + H^+]

Table 6.1 : Screening of reaction conditions for the reaction of 4-$PnNO_2$ and 3-PyOH

Entry	**Pre-treatment**	**V(µL) DMSO**	**Eq. K_2CO_3**	**Time (min)**	η **(µL/mg)**	**Average Conv. (%)**
1	no	0	0	30	0	0
2	no	0	1.5	30	0	14
3	no	0	3	30	0	4 ± 0
4	no	0	10	30	0	2
5	yes	10	3	45	0.013	28 ± 8
6	yes	25	1.5	45	0.045	9 ± 9
7	no	25	3	15	0.031	74 ± 26
8	no	25	3	30	0.031	43 ± 51
9	yes	25	3	30	0.031	81 ± 10
10	yes	25	3	45	0.031	96 ± 3
11	yes	25	10	45	0.013	51 ± 9
12	yes	50	3	45	0.063	92 ± 5

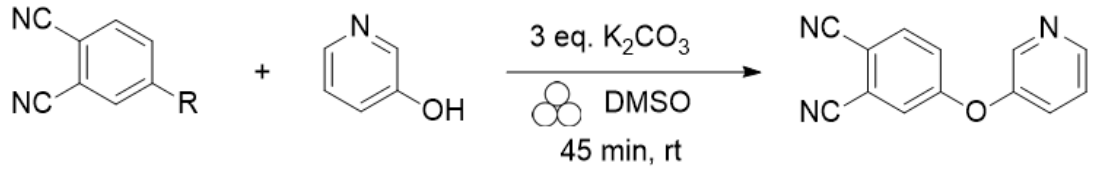

Table 6.2: Leaving group reactivity under optimized conditions

Entry	-R	V (µL) DMSO	η (µL/mg)	Conversion (%)
13	-I	25	0.042	0
14	-Br	25	0.036	0
15	-Br	100	0.192	0
16	-Cl	100	0.161	0
17	-F	25	0.056	1
18	-F	50	0.111	5
19*	-F	100	0.216	98
20*	-F	100	0.216	99

* 3-hydroxypiridine (1.2 eq), zirconium jar with zirconium ball.

4-(4-oxopyridin-1(4H)-yl)phthalonitrile (2)

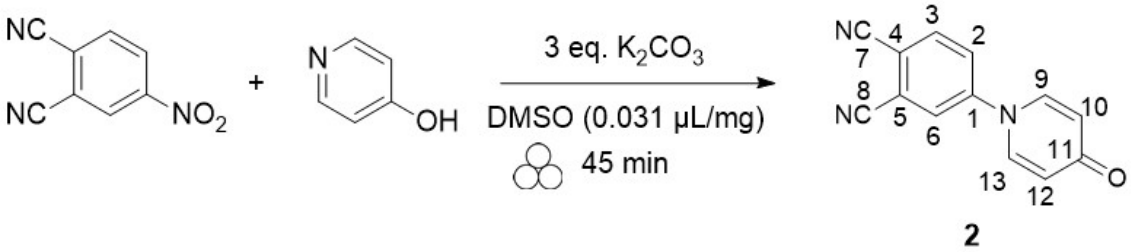

2

Synthesized from 4-nitrophthalonitrile (200 mg, 1.16 mmol) and 4-hydroxypyridine (110 mg, 1.16 mmol) in the presence of dry K_2CO_3 (491 mg, 3.48 mmol, 3 eq) and 25 µL DMSO (0.031 µL/mg) according to the general procedure for S_NAr of phthalonitriles with no pre-treatment to avoid color change and extraction from 5% MeOH in dichloromethane affording the crude as a beige solid (91±5% conversion, 68% yield).

^{1}H NMR (400 MHz, d6-DMSO) δ = 8.49 (1H, d, H-6), 8.32 (1H, d, H-3), 8.15 (3H, d, H-2, H-9,13) , 6.30 (2H, d, H-10,12) ppm. (**Figure A3**)

^{13}C NMR (101 MHz, d_6-DMSO) δ = 178.1 (C-11), 146.0 (C-1), 139.5 (C-9,13), 136.1 (C-3), 128.1 (C-6), 127.6 (C-2), 118.8 (C-10,12), 116.7 (C-7), 116.0 (C-8), 115.8 (C-5), 113.2 (C-4) ppm. (**Figure A4**)

ESI-MS: m/z calculated for $C_{13}H_7N_3O$: 221.1; found 222.1 [M + H^+]

4-(2-oxopyridin-1(2H)-yl)phthalonitrile (3)

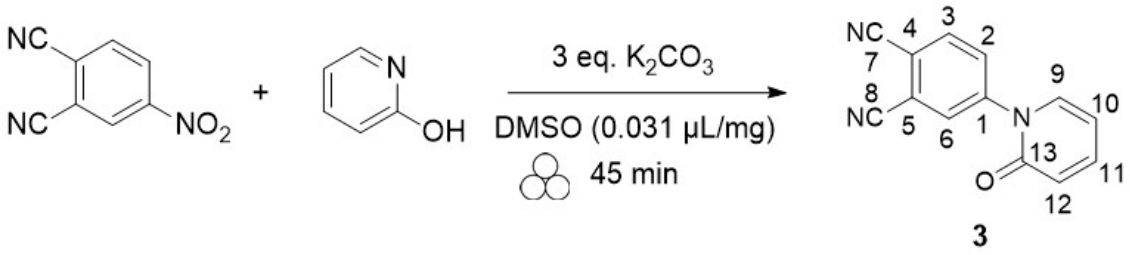

3

Synthesized from 4-nitrophthalonitrile (200 mg, 1.16 mmol) and 2-hydroxypyridine (110 mg, 1.16 mmol) in the presence of dry K_2CO_3 (491 mg, 3.48 mmol, 3 eq) and 25 µL DMSO (0.031 µL/mg) according to the general procedure for S_NArof phthalonitriles with extraction from 5% MeOH in dichloromethane affording the crude as a beige solid (82±11% conversion, 65% yield).

^{1}H NMR (400 MHz, d6-DMSO) δ = 8.38 (1H, d, H-6), 8.30 (1H, d, H-3), 8.06 (1H, dd, H-2), 7.73 (1H, dd, H-9), 7.56 (1H, t, H-11) 6.55 (1H, d, H-12), 6.40 (1H, t, H-10) ppm. (**Figure A6**)

^{13}C NMR (101 MHz, d_6-DMSO) δ = 161.1 (C-13), 144.9 (C-1), 141.9 (C-11), 138.5 (C-9), 135.3 (C-3), 133.1 (C-6), 133.0 (C-2), 121.2 (C-12), 116.0 (C-8), 115.9 (C-7), 115.8 (C-4), 114.5 (C-5), 106.9 (C-10) ppm. (**Figure A7**)

ESI-MS: m/z calculated for $C_{13}H_7N_3O$: 221.1; found 222.1 [M + H^+]

4-([1,1':3',1"-terphenyl]-2'-yloxy)phthalonitrile (4)

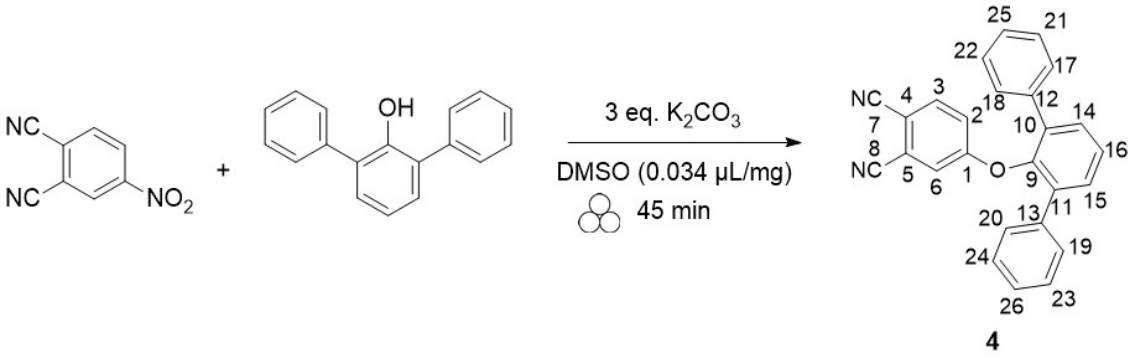

4

Synthesized from 4-nitrophthalonitrile (150 mg, 0.866 mmol) and 2,6-diphenylphenol (213 mg, 0.866 mmol) in the presence of dry K_2CO_3 (359 mg, 2.60 mmol, 3 eq) and 25 µL DMSO (0.034 µL/mg) according to the general procedure for S_NAr of phthalonitriles affording the crude as a beige solid (98±1% conversion, 95% yield)

^{1}**H NMR** (400 MHz, d6-DMSO) δ = 7.74 (1H, d, H-3), 7.56 (3H, t, H-6, H-14-15), 7.43 (4H, d, H-17-20), 7.37-7.31 (5H, m, H-16, H-21-25), 7.27 (2H, d, H-25-26) 6.97 (1H, dd, H-2) ppm. (**Figure A9**)

^{13}**C NMR** (101 MHz, d_6-DMSO) δ = 160.9 (C-1), 147.0 (C-9), 136.9 (C-12-13), 136.1 (C-3), 135.6 (C-10-11), 131.6 (C-6), 129.4 (C-17-20), 128.8 (C-21-24), 128.2 (C-25-26), 127.8 (C-14-15), 121.5 (C-16), 120.9 (C-2), 116.4 (C-7), 116.1 (C-8), 115.6 (C-5), 107.5 (C-4) ppm. (**Figure A10**)

ESI-MS: m/z calculated for $C_{26}H_{16}N_2O$: 372.13; [M] not found, decomoposes

4-((2-(dimethylamino)ethyl)thio)phthalonitrile (6)

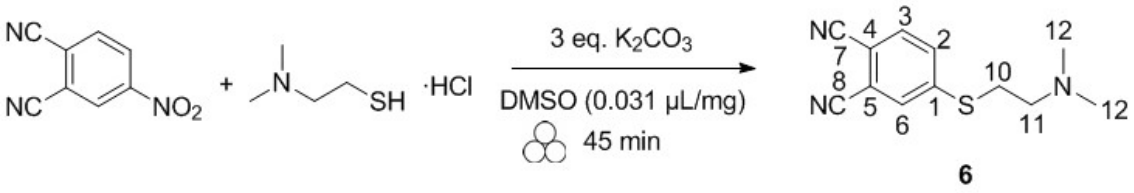

Synthesized from 4-nitrophthalonitrile (200 mg, 1.16 mmol) and 2-(dimethylamino)ethane thiol hydrochloride (122 mg, 1.16 mmol) in the presence of dry K_2CO_3 (479 mg, 3.47 mmol, 3 eq) and 25 µL DMSO (0.031 µL/mg) according to the general procedure for S_NAr of phthalonitriles with no pretreatment, affording the crude as a black solid (61±2% conversion, 64% yield).

^{1}H NMR (400 MHz, d6-DMSO) δ = 8.03 (1H, d, H-6), 7.96 (1H, d, H-2), 7.75 (1H, dd, H-3), 3.26 (2H, t, H-10), 2.54 (2H, t, H-11), 2.18 (6H, s, H-12) ppm. (**Figure A11**) Note: since this was a crude, the spectra present peaks from starting nitrophthalonitrile, only peaks belonging to the product are reported. The peaks of H-10 and H-11 slightly overlap with the water and solvent peak respectively, leading to slightly altered integrals.

^{13}C NMR (101 MHz, d_6-DMSO) δ = 147.6 (C-1), 134.1 (C-2), 130.9 (C-6), 130.8 (C-3), 116.6 (C-7), 116.2 (C-8), 115.5 (C-5), 110.0 (C-4), 57.2 (C-11), 45.2 (C-10), 29.6 (C-12) ppm. (**Figure A12**). Note: since this was a crude the spectra present peaks from starting nitrophthalonitrile, only peaks belonging to the product are reported.

ESI-MS: m/z calculated for $C_{12}H_{13}N_3S$: 231.1; found 232.1 [M + H^+]

3-(pyridin-3-yloxy)phthalonitrile (7)

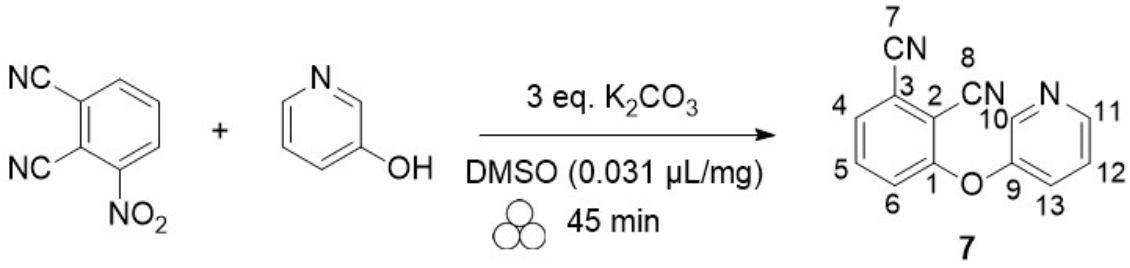

7

Synthesized from 3-nitrophthalonitrile (200 mg, 1.16 mmol) and 3-hydroxypyridine (110 mg, 1.16 mmol) in the presence of 3 eq. K_2CO_3 and 25 µL DMSO (0.031 µL/mg) for 45 minutes according to the general procedure for S_NAr of phthalonitriles affording the crude as a brown solid (97±3% conversion, 85% yield).

^{1}H NMR (400 MHz, d6-DMSO) δ = 8.59 (2H, dd, H-10-11), 7.88 (2H, m, H-4-5), 7.74 (1H, m, H-13), 7.56 (1H, m, H-12), 7.41 (1H, d, H-6) ppm. (**Figure A13**)

^{13}C NMR (101 MHz, d_6-DMSO) δ = 159.6 (C-1), 151.6 (C-9), 147.3 (C-11), 142.4 (C-10), 136.7 (C-5), 129.3 (C-4), 128.1 (C-13), 125.6 (C-12), 122.9 (C-6), 116.5 (C-3), 116.1 (C-7), 113.7 (C-8), 106.2 (C-2) ppm. (**Figure A14**)

ESI-MS: m/z calculated for $C_{13}H_7N_3O$: 221.1; found 222.1 [M + H^+]

4-chloro-5-(pyridin-3-yloxy)phthalonitrile (8)

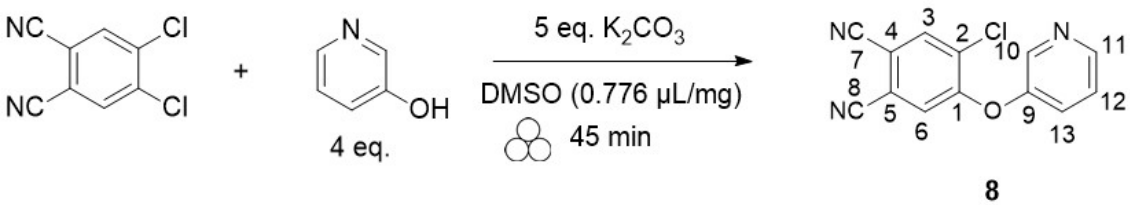

8

Synthesised from 4,5-dichlorophthalonitrile and 3-hydroxypyridine (2.2-4 eq.), in the presence of 5 equivalents of dry K_2CO_3 and DMSO according to the general procedure for S_NAr of phthalonitriles affording the mono-pyridyloxy in the crude as a

white solid (Conversions in **Table 6.3**, 96% yield)

^{1}H NMR (400 MHz, d6-DMSO) δ = 8.59 (1H, s, H-3), 8.52 (2H, m, H-10-11), 7.90 (1H, s, H-6), 7.67 (1H, dd, H-13), 7.55 (1H, dd, H-12) ppm. (**Figure A15**)

^{13}C NMR (101 MHz, d_6-DMSO) δ = 156.4 (C-1), 151.6 (C-9), 147.1 (C-10), 141.8 (C-11), 136.8 (C-3), 130.0 (C-2), 127.5 (C-13), 125.7 (C-12), 124.1 (C-6), 116.0 (C-7), 115.4 (C-8), 115.3 (C-5), 111.8 (C-4) ppm. (**Figure A16**)

ESI-MS: m/z calculated for $C_{13}H_6ClN_3O$: 255.0; found 256.0 [M + H^+]

Table 6.3: Optimization for reaction between 4,5-dichlorophthalonitrile and 3-PyOH

Entry	**Eq. 3-PyOH**	**Eq. K_2CO_3**	**V (µL) DMSO**	η **(µL/mg)**	**Conversion (%)**
21	2.2	6	30	0.024	23
22	2.2	6	50	0.039	39
23	4	5	25	0.039	6
24	4	5	50	0.078	24
25	4	5	500	0.775	94

4,5-bis(pyridin-3-yloxy)phthalonitrile (9)

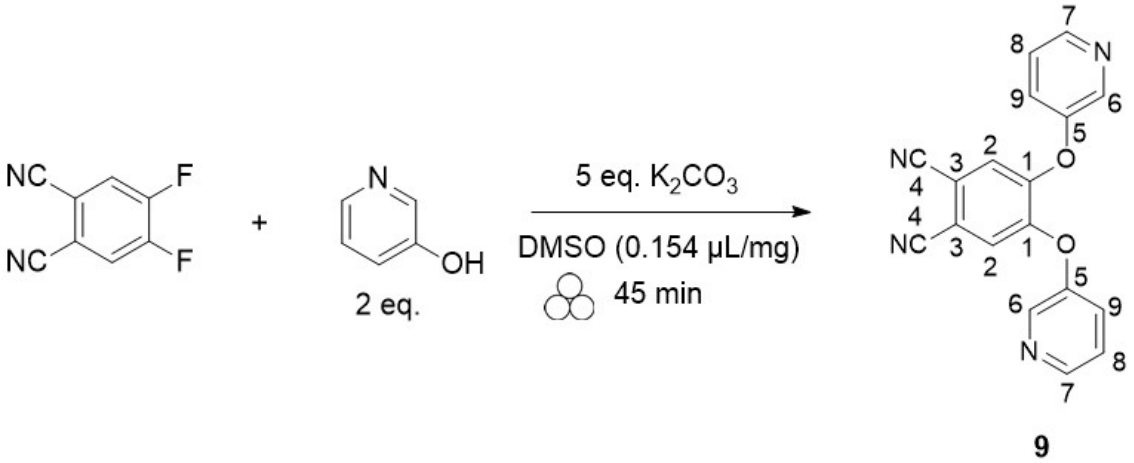

9

Synthesised from 4,5-difluorophthalonitrile (100 mg, 0.61 mmol) and 3-hydroxypyridine (128 mg, 1.34 mmol, 2.2 eq.), in the presence of dry K_2CO_3 (421 mg, 5 eq.) and 100 µL DMSO (0.154 µL/mg) according to the general procedure for S_NAr of phthalonitriles without pretreatment to avoid decomposition and in zirconium jars. The crude was purified by column (EtOAc:Hex 3:1) affording the pure bis-pyridiniloxy (78 mg, 42% yield)

^{1}**H NMR** (400 MHz, d6-DMSO) δ = 8.44 (4H, m, H-6,7), 8.05 (2H, s, H-2), 7.58 (2H, m, H-9), 7.46 (2H, m, H-8) ppm. (**Figure A17**)

^{13}**C NMR** (101 MHz, d_6-DMSO) δ = 152.2 (C-1), 150.8 (C-5), 146.4 (C-6), 141.0 (C-7), 126.4 (C-2), 126.3 (C-9), 125.4 (C-8), 115.7 (C-4), 112.2 (C-3) ppm. (**Figure A18**)

ESI-MS: m/z calculated for $C_{18}H_{10}N_4O_2$: 314.1; found 314.8 [M + H^+]

3,4,5,6-tetrakis(pyridin-3-yloxy)phthalonitrile (10)

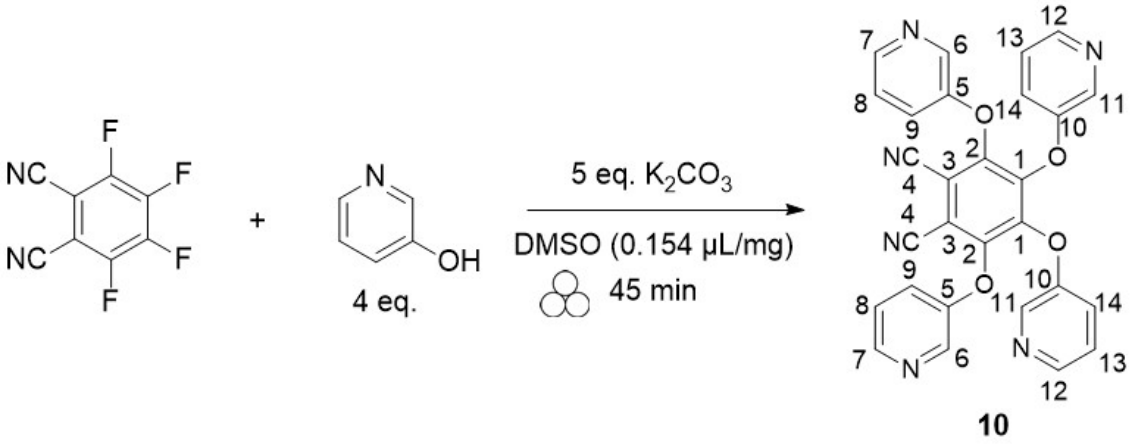

Synthesised from 4,5-tetrafluorophthalonitrile (50 mg, 0.25 mmol) and 3-hydroxypyridine (105 mg, 1.1 mmol, 4.4 eq.), in the presence of dry K_2CO_3 (345 mg, 10 eq.) and 100 µL DMSO (0.200 µL/mg) according to the general procedure for SNAr of phthalonitriles without pretreatment to avoid decomposition and milled with zirconium jars. The crude was purified by column (DCM:MeOH 90:10) affording the pure tetrakis-pyridiniloxy phthalonitrile (70 mg, 56% yield)

^{1}**H NMR** (400 MHz, d6-DMSO) δ = 8.42 (2H, d, H-6), 8.35 (2H, dd, H-7), 8.23 (2H, m, H-12), 8.02 (2H, m, H-11), 7.59 (2H, m, H-9), 7.40 (2H, m, H-8), 7.25 (4H, m, H-13-14) ppm. (**Figure A20**)

^{13}**C NMR** (101 MHz, d_6-DMSO) δ = 153.4 (C-5), 152.3 (C-10), 148.7 (C-1), 146.0 (C-7), 145.8 (C-2), 145.7 (C-12), 138.4 (C-6), 138.0 (C-11), 125.0 (C-8), 124.7 (C-14), 123.7 (C-9), 123.2 (C-13), 112.6 (C-4), 109.1 (C-3) ppm. (**Figure A21**)

ESI-MS: m/z calculated for $C_{28}H_{16}N_6O_4$: 500.1; found 500.7 [M + H^+]

General procedure for the synthesis of phthalocyanines

Phthalonitrile, $Zn(OAc)_2$ (0.5 eq.) and DMAE (0.177-0.198 µL/mg) were placed in a stainless steel jar with a single stainless steel ball. The mixture was milled for 5 minutes at 30 Hz. The resulting paste-like mixture was placed in the oven at 120 °C for 48 h. The mixture started to change color into a deep blue after an hour. The crude was washed with water and analysed without further purification.

[2,(3),9,(10),16,(17),23,(24)-tetrakis(pyridyl-3-oxy)phthalocyaninato]zinc(II) (11)

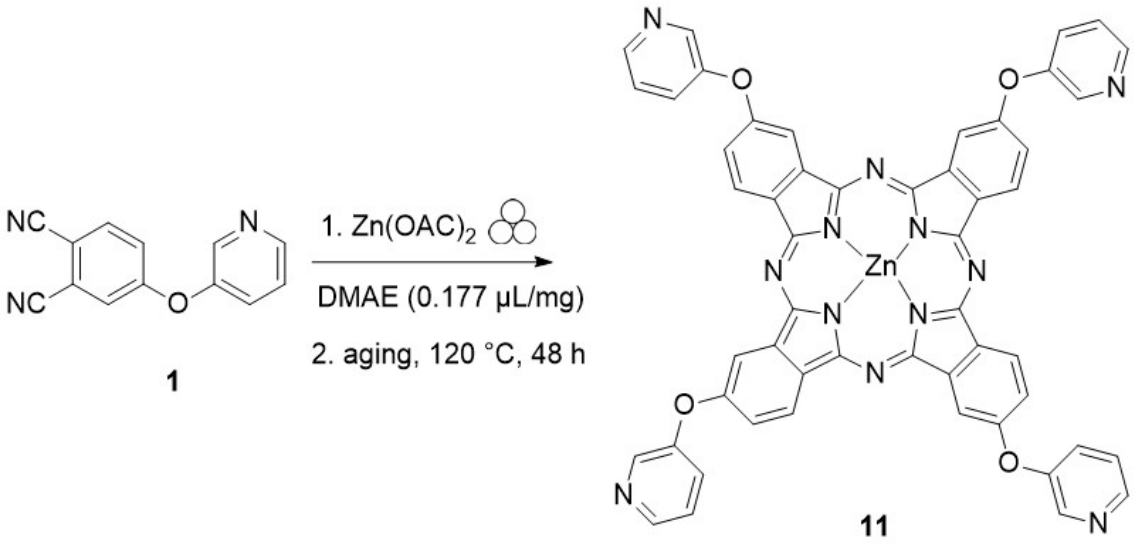

Synthesised from **1** (200 mg, 0.90 mmol) and zinc acetate (83 mg, 0.45 mmol) in the presence of 50 µL DMAE (0.177 µL/mg) according to the general procedure affording a deep blue solid.

^{1}**HNMR**: (**Figure A23**) in Appendix

MALDI-TOF: m/z calculated for $C_{52}H_{30}N_{12}O_4Zn$: 950.26; found 950.29 (**Figure A24**)

2,9(10),16(17),23(24)-tetrakis(4-oxopyridin-1(4H)-yl)-phthalocyaninatozinc(II) (12)

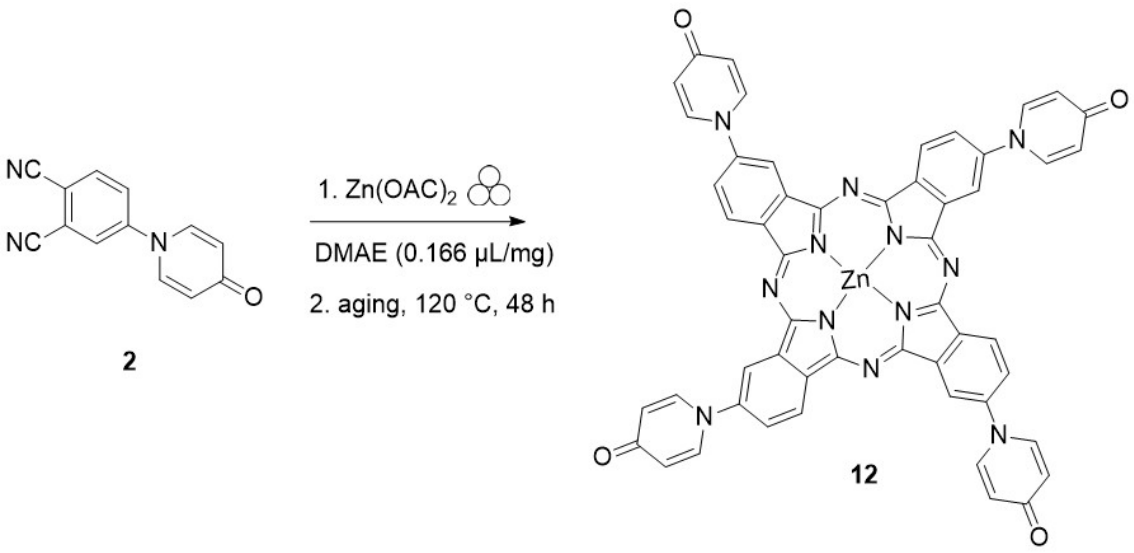

Synthesised from **2** (110 mg, 0.50 mmol) and zinc acetate (50 mg, 0.27 mmol) in the presence of 25 µL DMAE (0.166 µL/mg) according to the general procedure affording a deep blue solid.

^{1}**HNMR**: (**Figure A25**) in Appendix

MALDI-TOF: m/z calculated for $C_{52}H_{30}N_{12}O_4Zn$: 950.26; found 950.40, m/z calculated for $C_{52}H_{30}N_{12}O_4ZnNa$: 973.25; found 973.45 [M + Na^+] (**Figure A26**)

1,8(11),15(18),22(25) -tetrakis(pyridyl-3-oxy)phthalocyaninato]zinc(II) (14)

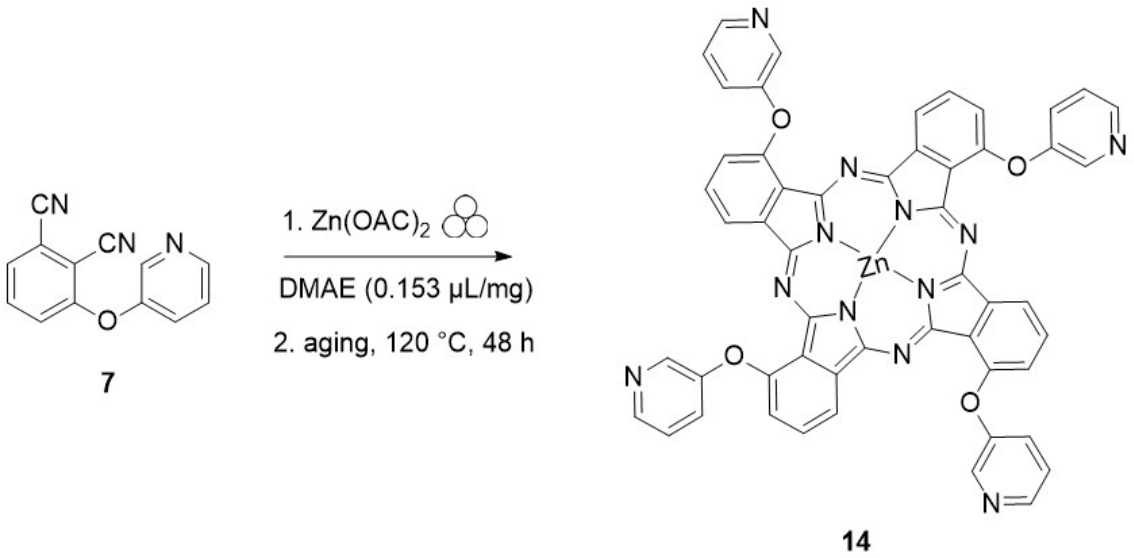

Synthesised from **7** (110 mg, 0.50 mmol) and zinc acetate (50 mg, 0.27 mmol) in the presence of 25 µL DMAE (0.153 µL/mg) according to the general procedure affording a deep blue solid.

^{1}**HNMR**: (**Figure A27**) in Appendix

MALDI-TOF: m/z calculated for $C_{52}H_{30}N_{12}O_4Zn$: 950.26; found 950.30 (**Figure A28**)

(1,2,3,4,8,9,10,11,15,16,17,18,22,23,24,25-hexadeca(pyridyl-3-oxy) phthalocyaninato)zinc(II) (15)

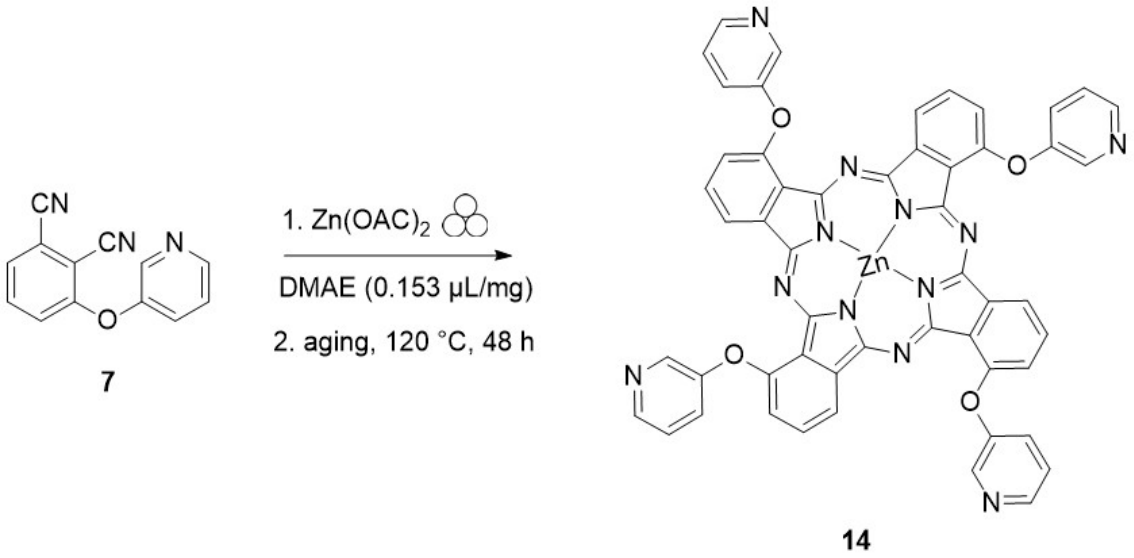

Synthesised from **10** (30 mg, 0.07 mmol) and zinc acetate (7 mg, 0.05 mmol) in the presence of 7 µL DMAE (0.193 µL/mg) according to the general procedure without pre-milling and aging for 72 hours, affording a deep green solid.

MALDI-TOF: m/z calculated for $C_{112}H_{66}N_{24}O_{16}Zn$: 2067.28; found 2068.38 [M + H^+] (**Figure A29**)

Bibliography

1 Miller, J. D.; Baron, E. D.; Scull, H.; Hsia, A.; Berlin, J. C.; McCormick, T.; Colussi, V.; Kenney, M. E.; Cooper, K. D.; Oleinick, N. L., *Toxicology and applied pharmacology*, 2007, **224** (3), 290–299.

2 Yuen, A. P.; Jovanovic, S. M.; Hor, A.-M.; Klenkler, R. A.; Devenyi, G. A.; Loutfy, R. O.; Preston, J. S., *Solar Energy*, 2012, **86** (6), 1683–1688.

3 Claessens, C. G.; Hahn, U.; Torres, T., The Chemical Record, 2008, **8** (2), 75–97.

4 Sakamoto, K.; Ohno-Okumura, E., *Materials*, 2009, **2** (3), 1127–1179.

5 Ptaszek, M., *Progress in molecular biology and translational science*, 2013, **113**, 59-108

6 Zanotti, G.; Palmeri, F.; Raglione, V., *Chemistry – A European Journal*, 2024, **30** (44), e202400908.

7 Andersen, J. M., Starbuck, H. F., *The Journal of Organic Chemistry*, 2021 **86** (20), 13983-13989.

8 Braun, A.; Tcherniac, J. Über, *Berichte der deutschen chemischen Gesellschaft*, 1907, **40** (2), 2709–2714.

9 Linstead, R. P., *Journal of the Chemical Society*, **1934**, 1016-1017.

10 Toru, T.; Uchida, H.; Tanaka, H.; Yoshiyama, H.; Reddy, P. Y.; Nakamura, S., *Synlett* **2002** (10), 1649–1652.

11 Leznoff, C. C.; Hu, M.; Nolan., *Chemical Communications* **1996** (10), 1245–1246.

12 Bai, Q.-L.; Zhang, C.-H.; Song, J.-J.; Liu, J.-H.; Feng, Y.-C.; Duan, L.-M.; Cheng, C.-H., *Chinese Chemical Letters*, 2016, **27** (5), 764–768.

13 Lee, C.-H.; Ng, D. K. P., *Tetrahedron Letters*, 2002, **43** (23), 4211–4214.

14 Li, D.; Zhang, P.; Ge, S.; Sun, G.; He, Q.; Fa, W.; Li, Y.; Ma, J. A, *RSC Advances*, 2021, **11** (50), 31226–31234.

15 Ferreira, J. T.; Pina, J.; Alberto, C.; Fernandes, R.; João P. C. Tomé; M. Salomé Rodríguez-Morgade; Torres, T., *Journal of Materials Chemistry B 2017*, **5** (29), 5862–5869.

16 Zanotti, G.; Mancini, L.; Paoletti, A. M.; Pennesi, G.; Venanzio Raglione., *Journal of Porphyrins and Phthalocyanines*, 2022, **27** (01n04), 398–401.

17 Kharisov, B. I.; Medina, A. M.; Rivera, J.; U. Ortiz Méndez., *Journal of Chemical Research* **2005** (6), 404–406.

18 Youssef, T. E., *Polyhedron*, 2010, **29** (7), 1776–1783.

19 Sharma, R. K.; Gulati, S.; Pandey, A., *Inorganica Chimica Acta*, 2012, **397**, 21–31.

20 Podapangi, S. K.; Mancini, L.; Xu, J.; Reddy, S. H.; Di Carlo, A.; Brown, T. M.; Zanotti, G.,. *Energies* **2023**, 16 (9), 3643.

21 Ng, D. K.; Lo, P.-C.; Cheng, D. Y., *Synthesis*, **2005** (7), 1141–1147.

22 Shaabani, A.; Hooshmand, S. E.; Afshari, R.; Shaabani, S.; Ghasemi, V.; Atharnezhad, M.; Akbari, M., *Journal of Solid State Chemistry*, 2018, **258**, 536–542.

23 Zhu, L.; Jing, X.; Song, L.; Liu, B.; Zhou, Y.; Xiang, Y.; Xia, D., *New Journal of Chemistry*, 2013, **38** (2), 663–668.

24 Mayukh, M.; Sema, C. M.; Roberts, J. M.; McGrath, D. V., *The Journal of Organic Chemistry*, 2010, **75** (22), 7893–7896.

25 Wu, Y.; Jiang, Z.; Lu, X.; Liang, Y.; Wang, H., *Nature*, 2019, **575** (7784), 639–642.

26 Lokesh, K. S.; Adriaens, A. *Dyes and pigments*, 2013, **96** (1), 269–277.

27 Langerreiter, D.; Kostiainen, M. A.; Kaabel, S.; Anaya-Plaza, E., *Angewandte Chemie International Edition*, 2022, **61** (42), e202209033.

28 Fan, J.; Wang, T.; Thapaliya, B. P.; Qiu, L.; Li, M.; Wang, Z.; Kobayashi, T.; Popovs, I.; Yang, Z.; Dai, S., *Angewandte Chemie International Edition*, 2022, **61** (38).

29 Nemykin, V. N., Lukyanets, E. A., *ARKIVOC: Online Journal of Organic Chemistry*, **2010** (1), 136-208.

30 Lukyanets, E. A.; Nemykin, V. N., *Journal of Porphyrins and Phthalocyanines*, 2010, **14** (01), 1–40.

31 Rodríguez-Morgade, M. S., Torres, T. 17.9.24 Phthalocyanines and Related Compounds. *Science of Synthesis Knowledge Updates*; Thieme, 2017, Vol. 2, pp 1237-1352.

32 Beck, A.; Mangold, K.; Hanack, M. Lösliche, *Chemische Berichte*, 1991, **124** (10), 2315–2321.

33 Aranyos, V., Castano, A. M., Grennberg, H., *Acta Chemica Scandinavica*, 1999 **53**(9), 714-720.

34 Leznoff, C. C.; Hu, M.; Nolan., *Chemical Communications* **1996** (10), 1245–1246.

35 Maya, E. M.; Haisch, P.; Vázquez, P.; Torres, T., *Tetrahedron*, 1998, **54** (17), 4397–4404

36 Wöhrle, D.; Iskander, N.; G. Graschew; Sinn, H.; Friedrich, E. A.; W. Maier-Borst; Stern, J.; Schlag, P., *Photochemistry and Photobiology*, 1990, 51 (3), 351–356.

37 Gürol, İ., Ahsena, V., Bekaroğlu, Ö., *Journal of the Chemical Society, Dalton Transactions*, **1994** (4), 497-500.

38 Ağcaabat, R., Seslikaya, C., Fındık, V., Erdem, S. S., Odabaş, Z., *New Journal of Chemistry*, 2024, **48**(4), 1623-1633.

39 Atajanov, R., Huraibat, B., Odabaş, Z., Özkaya, A. R., *Inorganica Chimica Acta*, 2023, **547**, 121360.

40 Gonzalez, A. C., Damas, L., Aroso, R. T., Tome, V. A., Dias, L. D., Pina, J., Pereira, M. M., *Journal of Porphyrins and Phthalocyanines*, 2020 **24**(05n07), 947-958.

41 Lyubimtsev, A., Iqbal, Z., Crucius, G., Syrbu, S., Ziegler, T., Hanack, M., *Journal of Porphyrins and Phthalocyanines*, 2012, **16**(05n06), 434-463.

42 Choi, C. F., Huang, J. D., Lo, P. C., Fong, W. P., Ng, D. K., *Organic & Biomolecular Chemistry*, 2008, **6**(12), 2173-2181.

43 Cosimelli, B., Roncucci, G., Dei, D., Fantetti, L., Ferroni, F., Ricci, M., Spinelli, D., *Tetrahedron*, 2003, **59**(50), 10025-10030.

44 Znoiko, S. A., Kuzmina, M. S., Maizlish, V. E., Koshel, G. N., Lebedeva, N. V., *Russian Journal of General Chemistry*, 2023, **93**(7), 1736-1744.

45 Wang, J., Khanamiryan, A. K., Leznoff, C. C., *Journal of Porphyrins and Phthalocyanines*, 2004, **8**(11), 1293-1299.

46 Pasimeni, L., Meneghetti, M., Rella, R., Valli, L., Granito, C., Troisi, L., *Thin Solid Films*, 1995, **265**(1-2), 58-65.

47 Leznoff, C. C., Hu, M., McArthur, C. R., Qin, Y., van Lier, J. E., *Canadian journal of chemistry*, 1994, **72**(9), 1990-1998.

48 Gurol, I., Altinkok, C., Agel, E., Tasaltin, C., Durmuş, M., Acik, G., *Journal of Coatings Technology and Research*, 2020 **17**, 1587-1596.

49 Araújo, A. R., Tomé, A. C., Santos, C. I., Faustino, M. A., Neves, M. G., Simões, M. M., Cavaleiro, J. A., *Molecules*, 2020, **25**(7), 1745.

50 Sample, H. C.; Senge, M. O., *European Journal of Organic Chemistry*, 2020, **2021** (1), 7–42.

51 Lin, M. J., Wang, J. D., Chen, N. S., Huang, J. L., *Journal of Coordination Chemistry*, 2006, **59**(6), 607-611.

52 Leznoff, C. C., Sosa-Sanchez, J. L., *Chemical Communications*, **2004** (3), 338-339.

53 Leznoff, C. C., Hiebert, A., Ok, S., *Journal of Porphyrins and Phthalocyanines*, 2007, **11**(07), 537-546.

54 Aggarwal, A., Singh, S., Zhang, Y., Anthes, M., Samaroo, D., Gao, R., Drain, C. M., *Tetrahedron Letters*, 2011, **52**(42), 5456-5459.

55 Lourenço, L. M., Neves, M. G., Cavaleiro, J. A., Tome, J. P., *Tetrahedron*, 2014 **70**(17), 2681-2698.

56 Takacs, L., *Chemical Society Reviews*, 2013, **42** (18), 7649–7659.

57 Takacs, L., *JOM*, 2000, **52** (1), 12–13.

58 Anastas, P. T.; Warner, J. C. *Green Chemistry: Theory and Practice*, Oxford University Press: New York, 1998, p.30

59 Gomollón-Bel, F., *Chemistry International*, 2019, **41**(2), 12-17.

60 Pagola, S., *Crystals*, 2023, **13** (1), 124.

61 Jafter, O. F.; Lee, S.; Park, J.; Cabanetos, C.; Lungerich, D., *Angewandte Chemie International Edition*, 2024, **63** (48).

62 Ying, P.; Yu, J.; Su, W., *Advanced Synthesis & Catalysis*, 2021, **363** (5), 1246–1271.

63 Wang, G.-W., Chemical Society Reviews 2013, **42** (18), 7668-7700.

64 Porcheddu, A.; Colacino, E.; De Luca, L.; Delogu, F., . *ACS Catalysis*, 2020, **10** (15), 8344–8394.

65 Pérez-Venegas, M., Juaristi, E., *ACS Sustainable Chemistry & Engineering*, 2020, **8**(24), 8881-8893.

66 Nielsen, S. F.; Peters, D.; Axelsson, O., *Synthetic Communications*, 2000, **30** (19), 3501–3509.

67 Thorwirth, R.; Stolle, A.; Ondruschka, B., *Green Chemistry*, 2010, **12** (6), 985-991.

68 Frejd, T.; Tullberg, E.; Schacher, F.; Peters, D., *Synthesis*, **2006**, 7, 1183–1189.

69 Raston, C. L.; Scott, J. L., *Green Chemistry*, 2000, **2** (2), 49–52.

70 Wang, G.-W.; Zhang, Z.; Dong, Y.-W.; Komatsu, K., *Synlett* **2004** (1), 61–64.

71 Kaupp, G.; Schmeyers, J.; Boy, J., *Chemosphere*, 2001, **43** (1), 55–61.

72 Thorwirth, R.; Stolle, A.; Ondruschka, B.; Wild, A.; Schubert, U. S., *Chemical Communications*, 2011, **47** (15), 4370-4372

73 Mashkouri, S.; Reza Naimi-Jamal, M., 2009, **14** (1), 474–479.

74 Dong, Y.-W.; Wang, G.-W.; Wang, L., *Tetrahedron*, 2008, **64** (44), 10148–10154.

75 Balema, V.; P., Wiench, J. W.; Pruski, M.; Pecharsky, V. K., *Journal of the American Chemical Society*, 2002, **124** (22), 6244-6245

76 Clayden, J.; Greeves, N.; Warren, S., *Organic Chemistry*, 2nd ed. Oxford University Press, 2012, p.515-520.

77 Sherwood, J., Albericio, F., de la Torre, B. G., *ChemSusChem*, 2024 **17**(8), e202301639.

78 Vaghi, L; Palomba, E.; Papagni, A., *RSC Mechanochemistry*, 2024, **1**, 342–348

79 Andersen, J.; Starbuck, H.; Current, T.; Martin, S.; Mack, J., *Green Chemistry*, 2021, **23** (21), 8501–8509.

80 Jakubczyk, M.; Mkrtchyan, S.; Mohanad Shkoor; Lanka, S.; Budzák, S.; Iliaš, M.; Skoršepa, M; Iaroshenko, V. O., *Journal of the American Chemical Society*, 2022, **144** (23), 10438–10445.

81 Mkrtchyan, S.; Purohit, V. B.; Shalimov, O.; Zapletal, J.; Sarfaraz, S.; Ayub, K.; Iaroshenko, V. O., *ACS Sustainable Chemistry & Engineering*, 2024, **12**(24), 8980-8989.

82 Mkrtchyan, S.; Purohit, V. B.; Zapletal, J.; Shalimov, O.; Nociarová, J.; Addová, G.; Filo, J.; Garcia, M. G.; Kupcová, E.; Benická, B.; Iaroshenko, V. O., *Cell Reports Physical Science*, 2024, **5** (8), 102118.

83 Rodrigo, E.; Wiechert, R.; Walter, M. W.; Braje, W.; Geneste, H., *Green Chemistry*, 2022, **24**(4), 1469–1473.

84 Leitch, J. A.; Smallman, H. R.; Browne, D. L., *The Journal of Organic Chemistry*, 2021, **86** (20), 14095–14101.

85 Sowa, A., Höing, A., Dobrindt, U., Knauer, S. K., Galstyan, A., Voskuhl, J., *Chemistry–A European Journal*, 2021, **27**(59), 14672-14680.

86 Mantareva, V., Angelov, I., Kussovski, V., Dimitrov, R., Lapok, L., Wöhrle, D., *European journal of medicinal chemistry*, 2011, **46**(9), 4430-4440.

87 Tasso, T. T., Furuyama, T., Kobayashi, N., *Inorganic chemistry*, 2013, **52**(16), 9206-9215.

7. Appendix

The ^{1}HNMR and ^{13}CNMR spectrum of the synthesised compounds are provided. All spectra are measured in d_6-DMSO at 23 °C. Only the aromatic regions are shown for clarity except when necessary. ^{19}FNMR spectrum comparisons are offered for **9** and **10**. MALDI spectra are presented for the phthalocyanines.

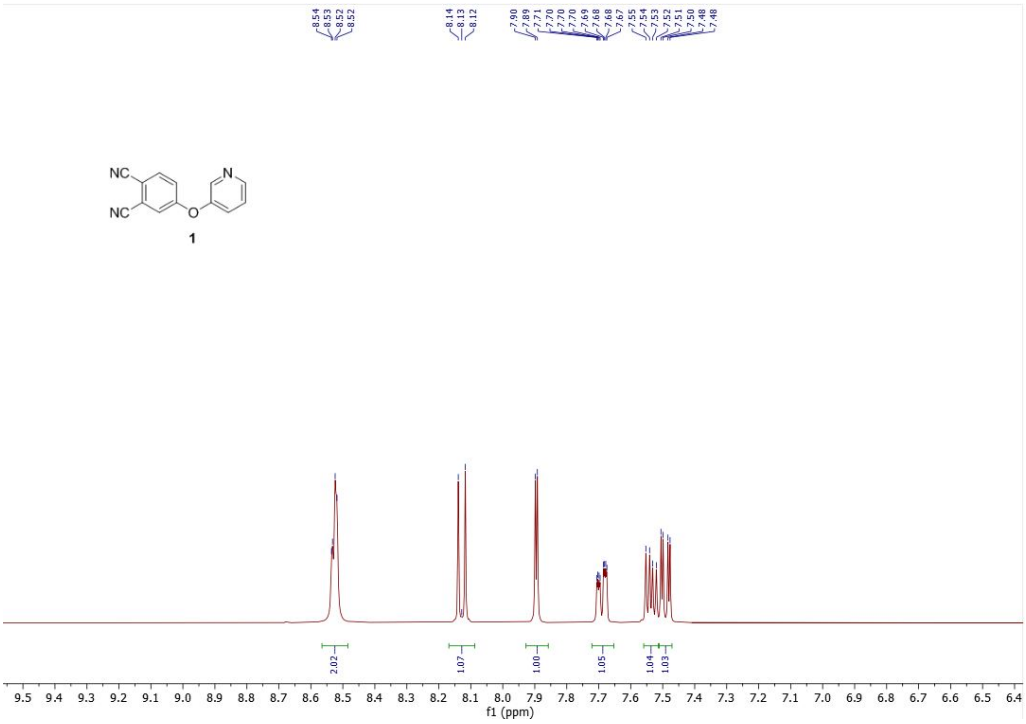

A1: ^{1}HNMR spectrum for compound **1**

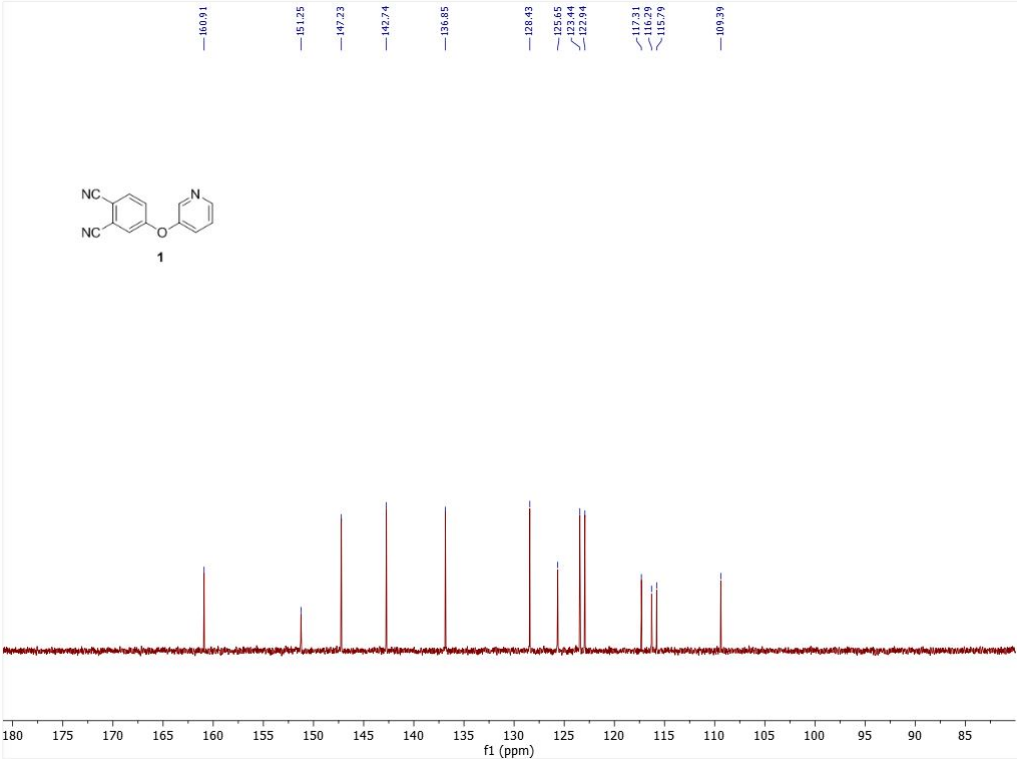

A2: ^{13}CNMR spectrum for compound **1**

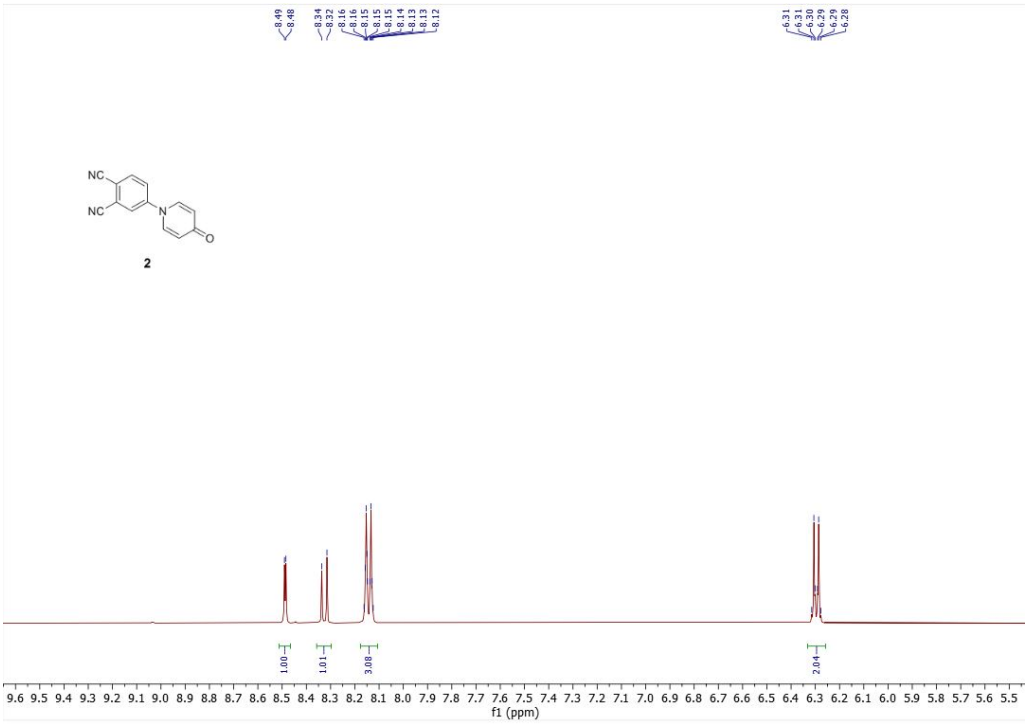

A3: ^{1}HNMR spectrum for compound **2**

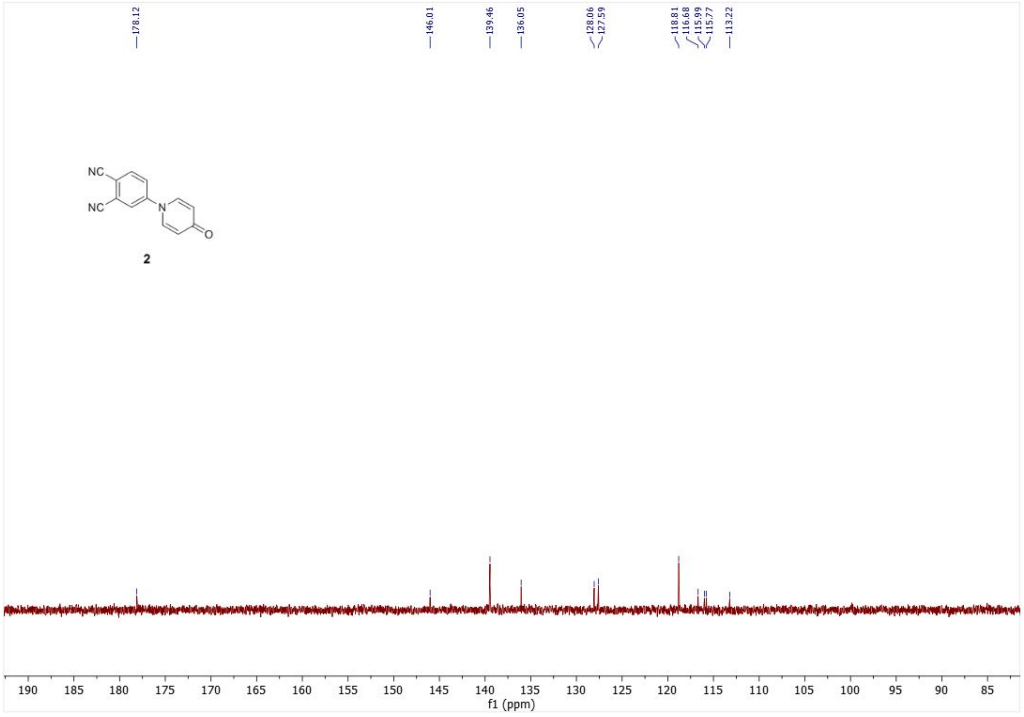

A4: ^{13}CNMR spectrum for compound **2**

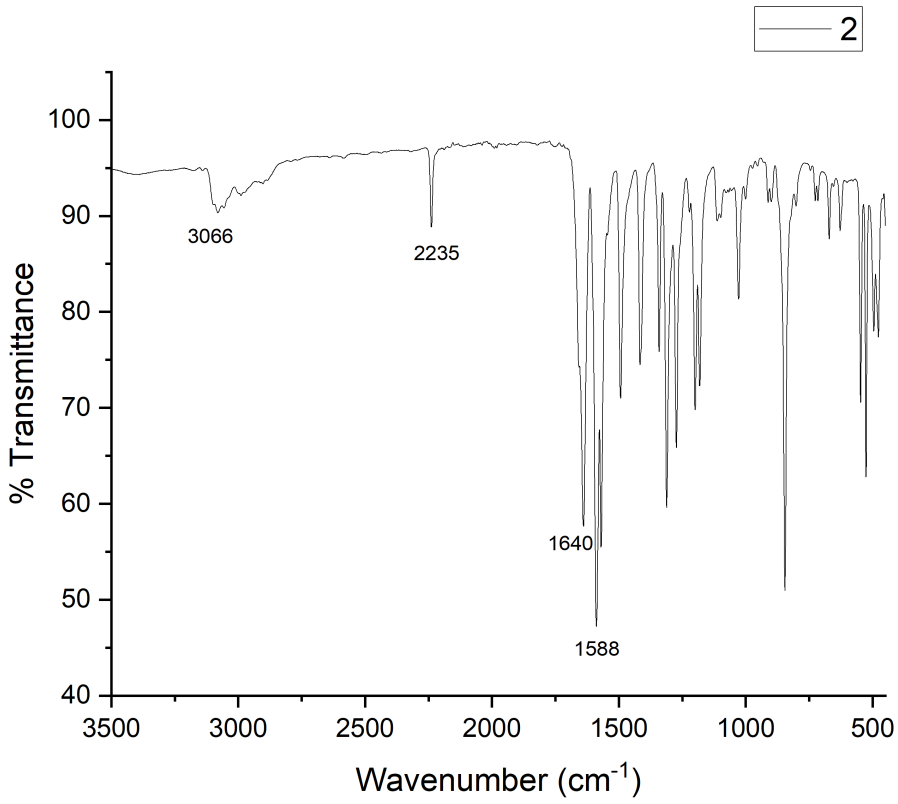

A5: IR spectrum for compound **2**

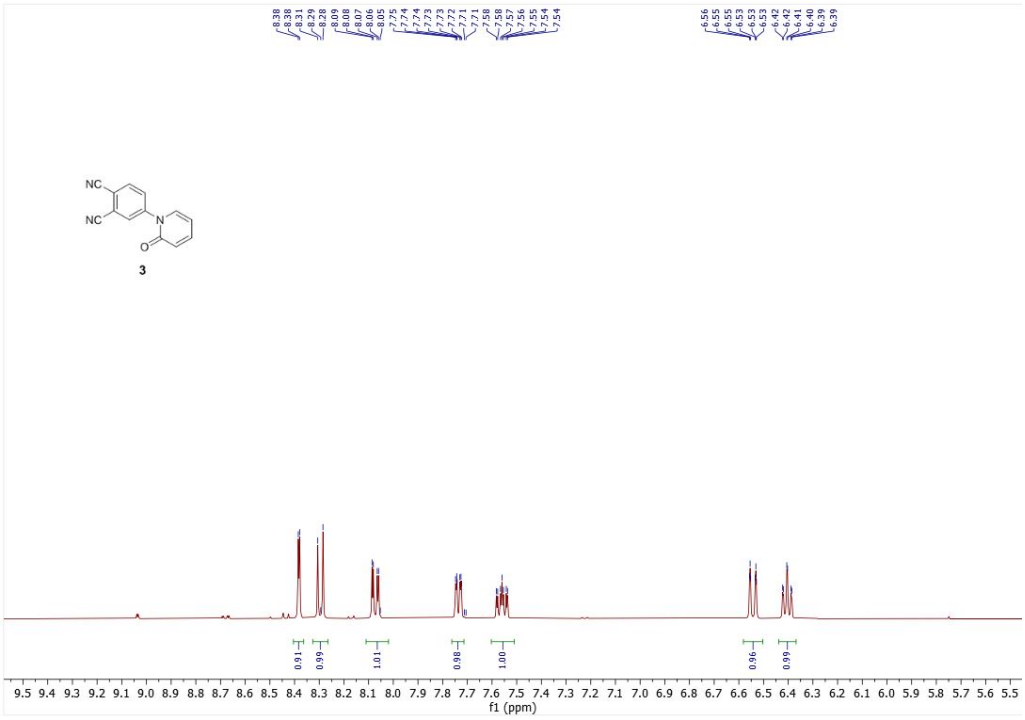

A6: ^{1}HNMR spectrum for compound **3**

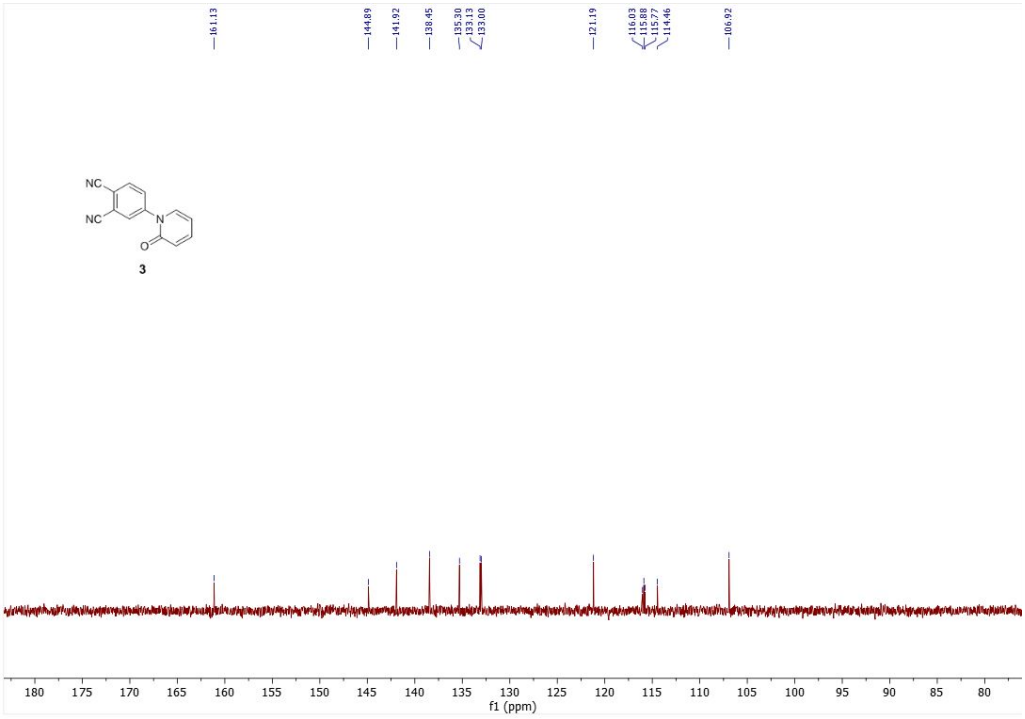

A7: ^{13}CNMR spectrum for compound **3**

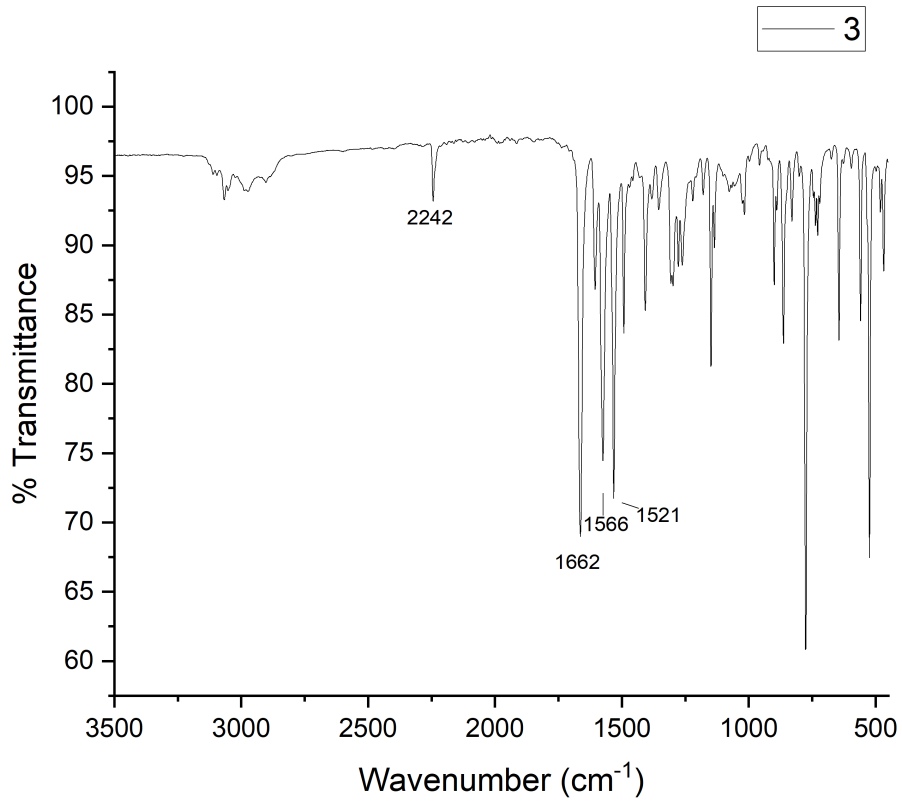

A8: IR spectrum for compound **3**

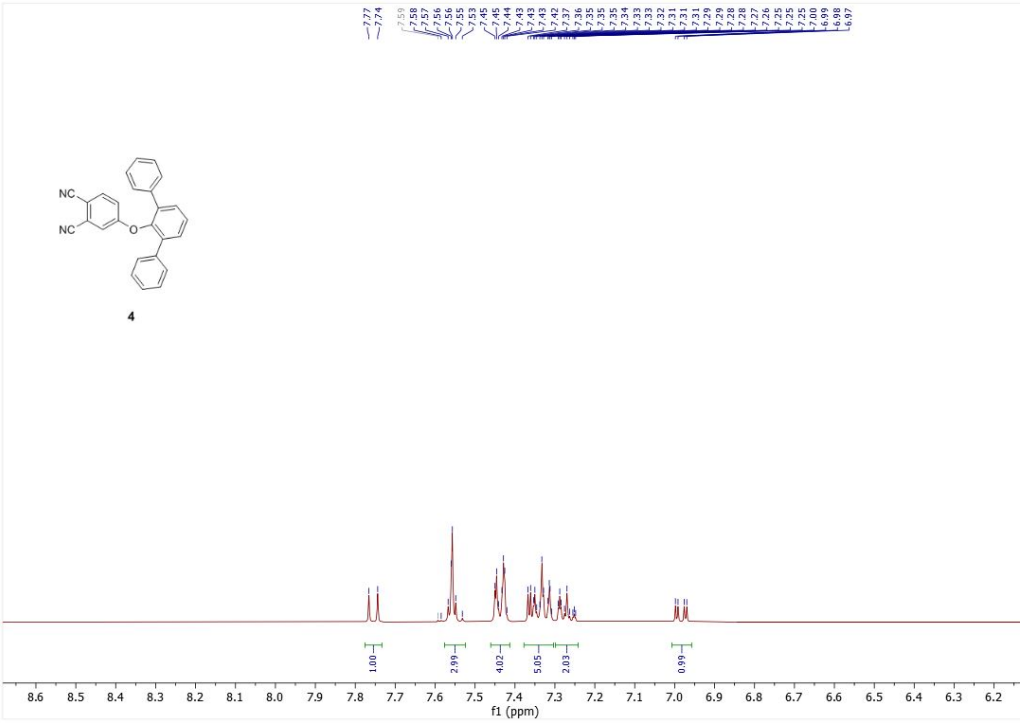

A9: ^{1}HNMR spectrum for compound **4**

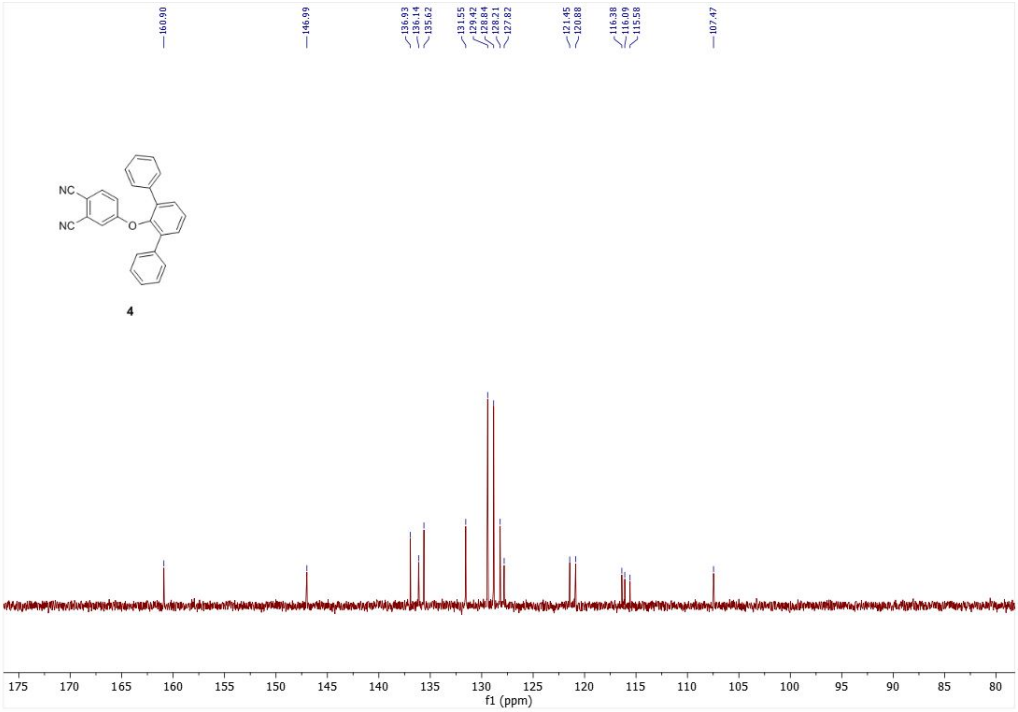

A10: ^{13}CNMR spectrum for compound **4**

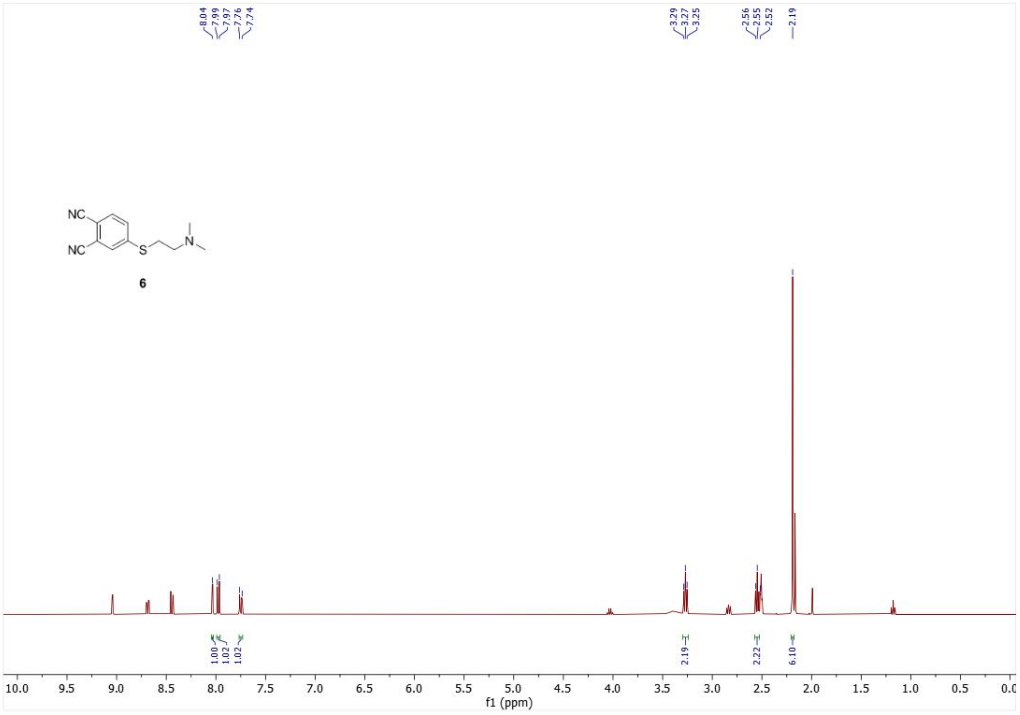

A11: ^{1}HNMR spectrum for compound **6**

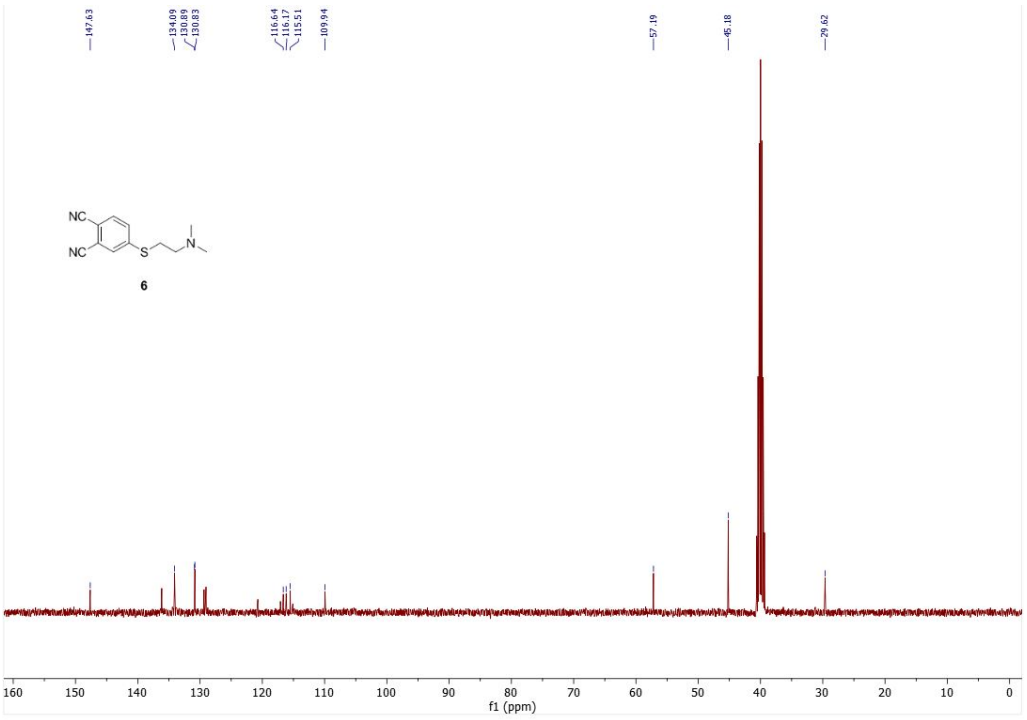

A12: ^{13}CNMR spectrum for compound **6**

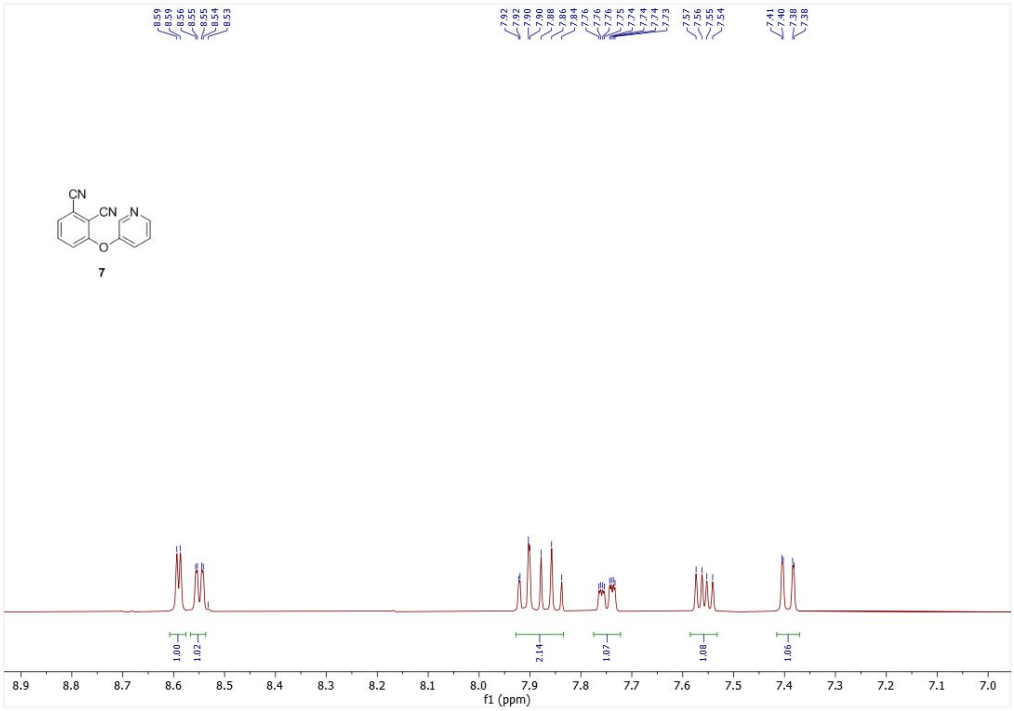

A13: ^{1}HNMR spectrum for compound **7**

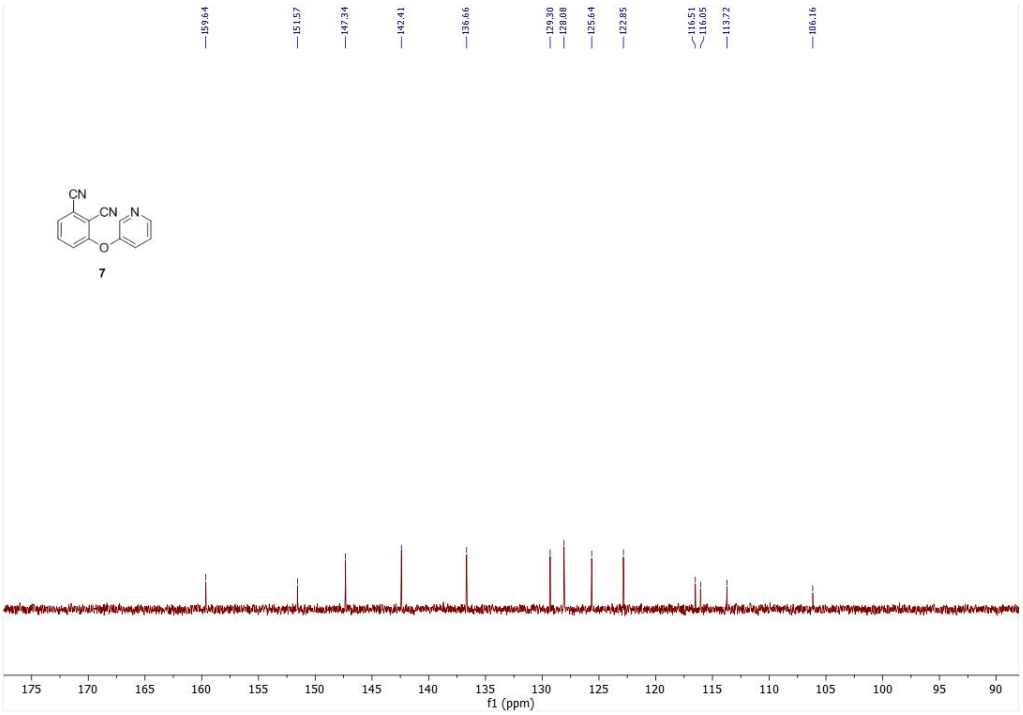

A14: ^{13}CNMR spectrum for compound **7**

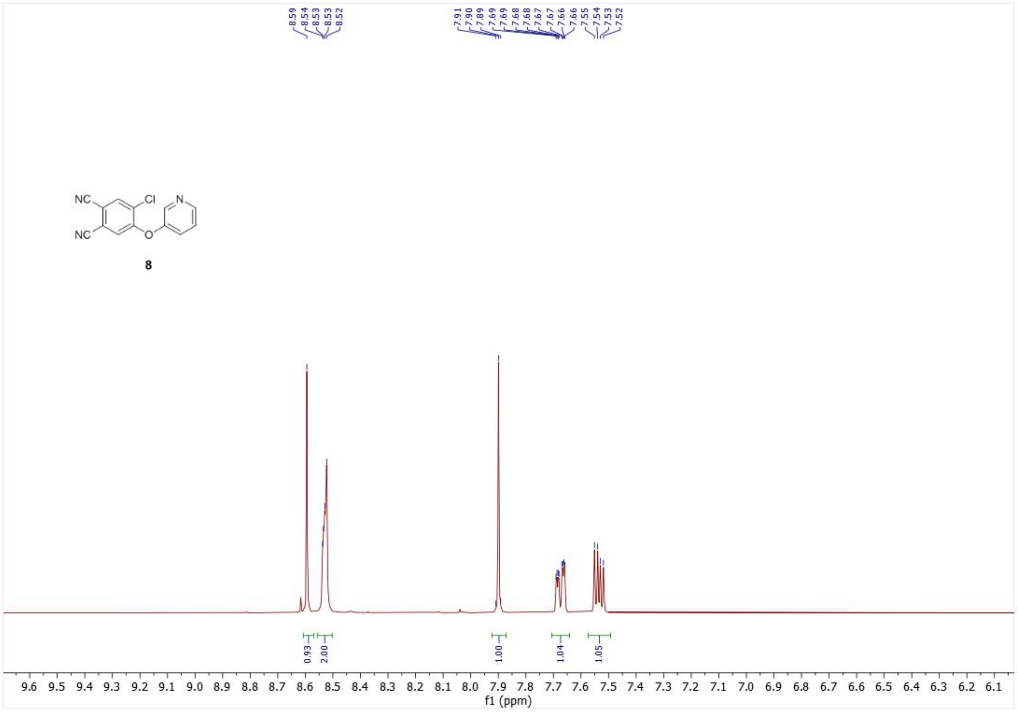

A15: ^{1}HNMR spectrum for compound **8**

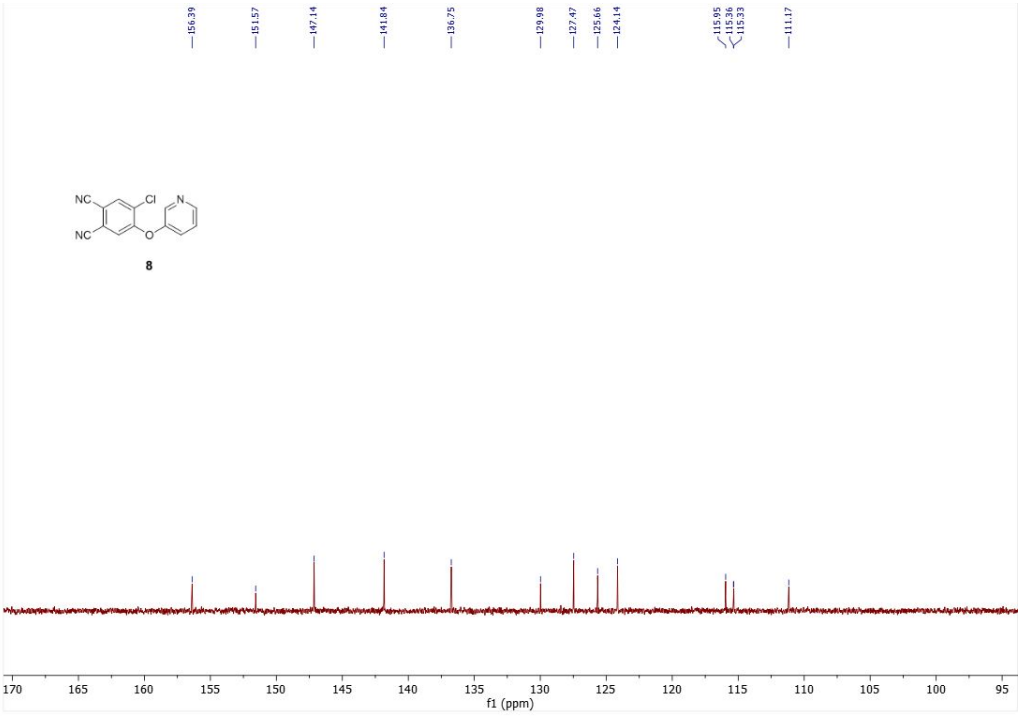

A16: ^{13}CNMR spectrum for compound **8**

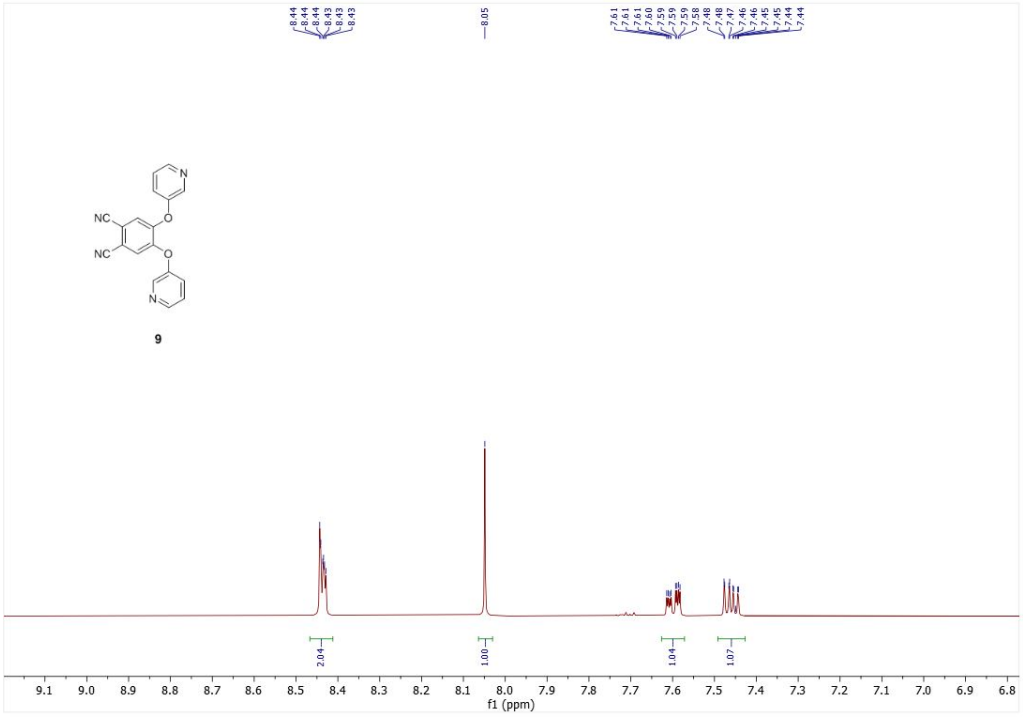

A17: ^{1}HNMR spectrum for compound **9**

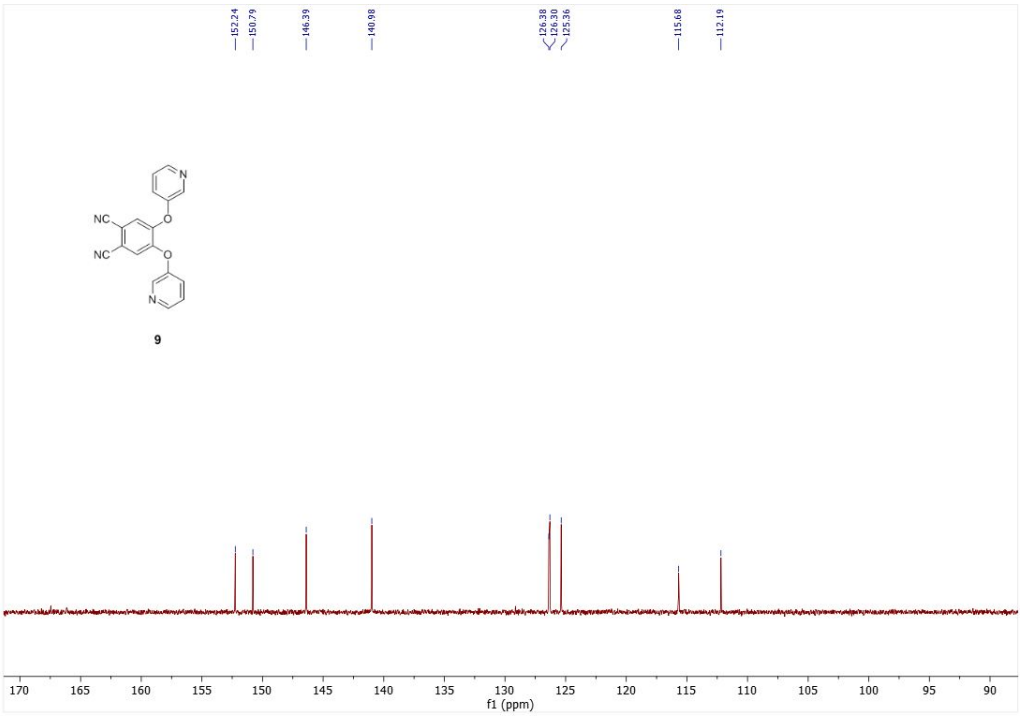

A18: ^{13}CNMR spectrum for compound **9**

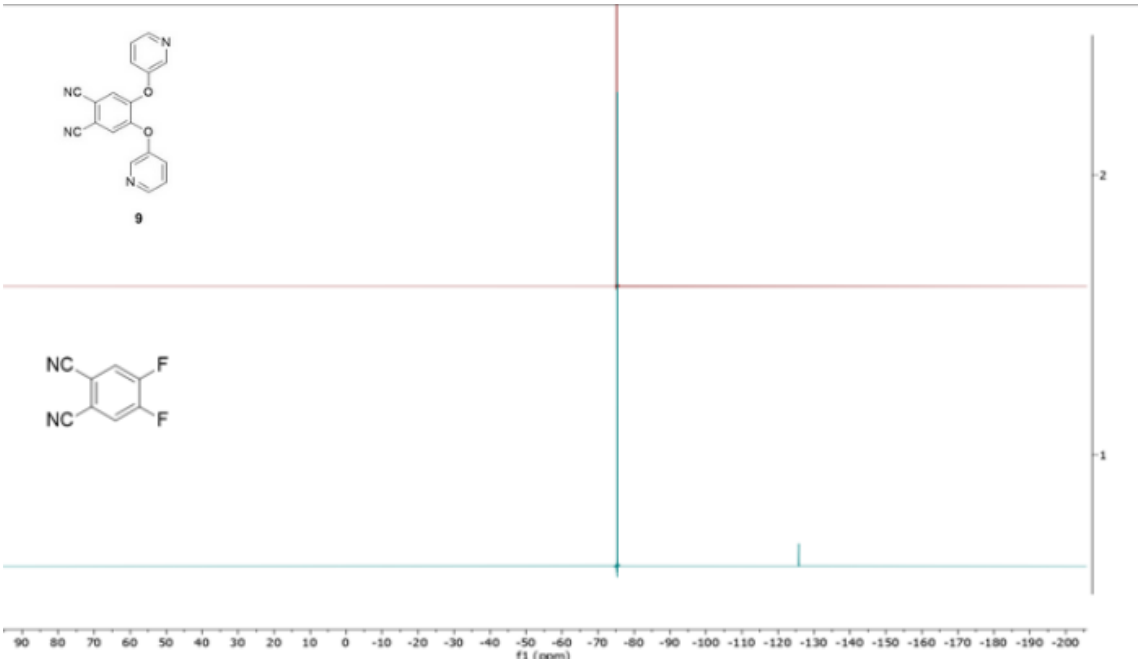

A19: ^{19}FNMR spectrum for compound **9** and 4,5-difluorophthalonitrile with trifuoroacetic acid (TFA) as standard.

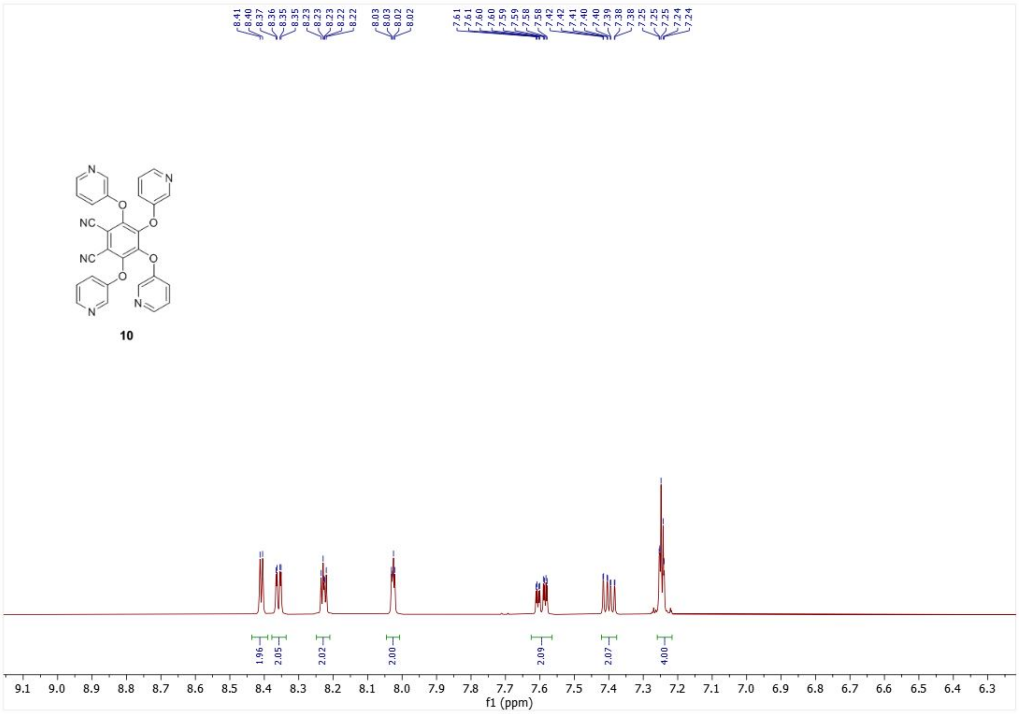

A20: ^{1}HNMR spectrum for compound **10**

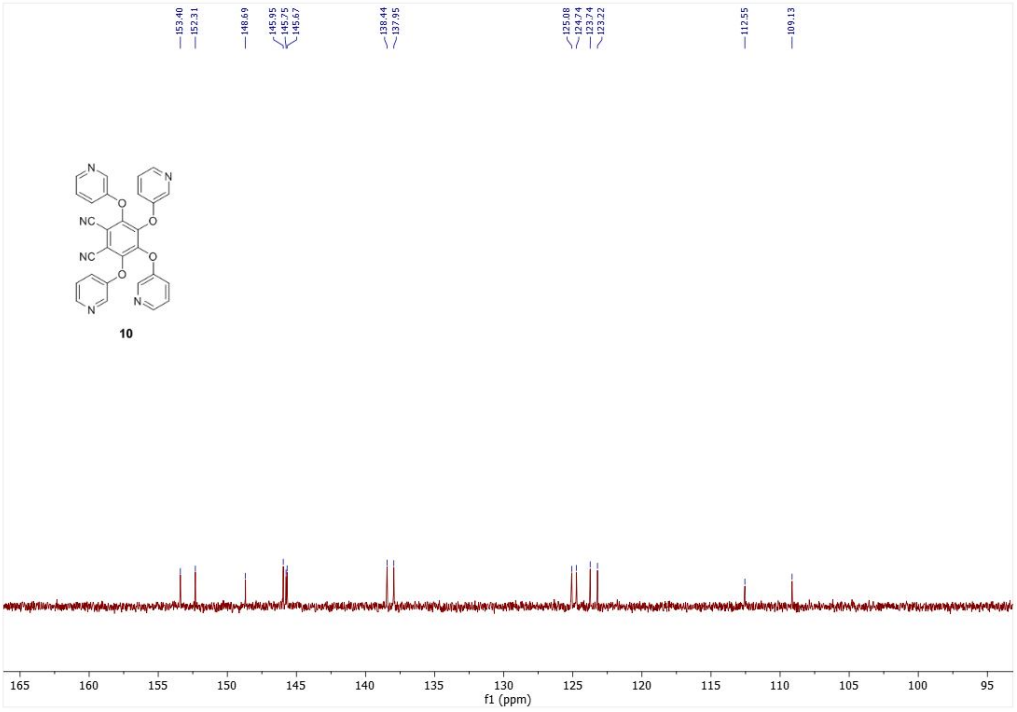

A21: ^{13}CNMR spectrum for compound **10**

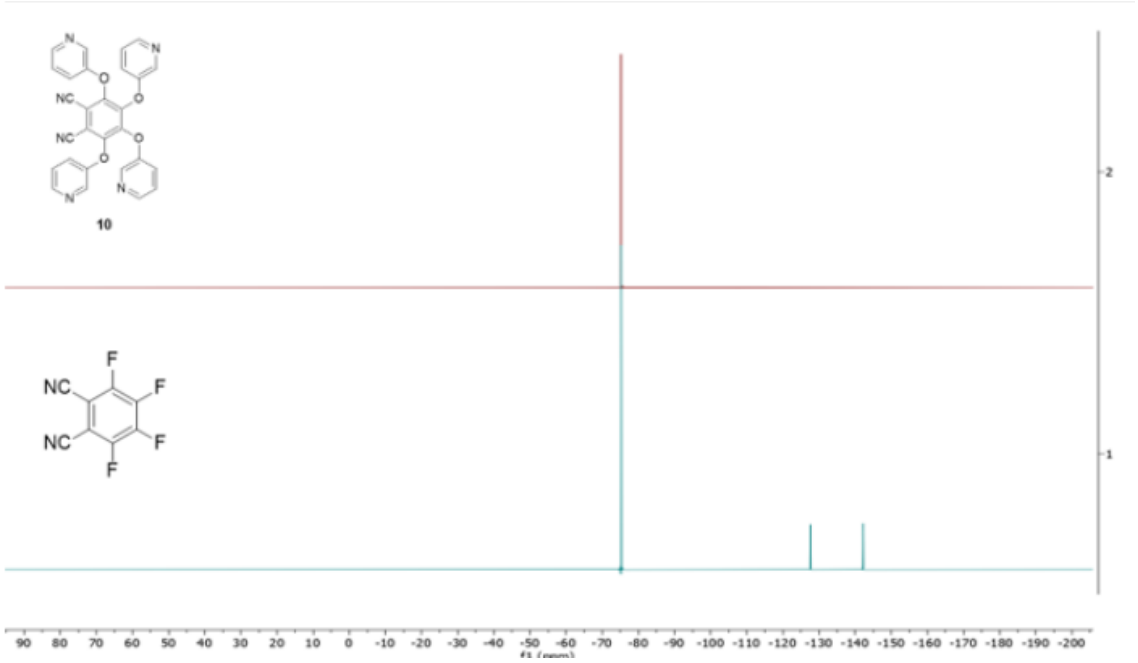

A22: ^{19}FNMR spectrum for compound **10** and tetrafluorophthalonitrile with TFA as standard.

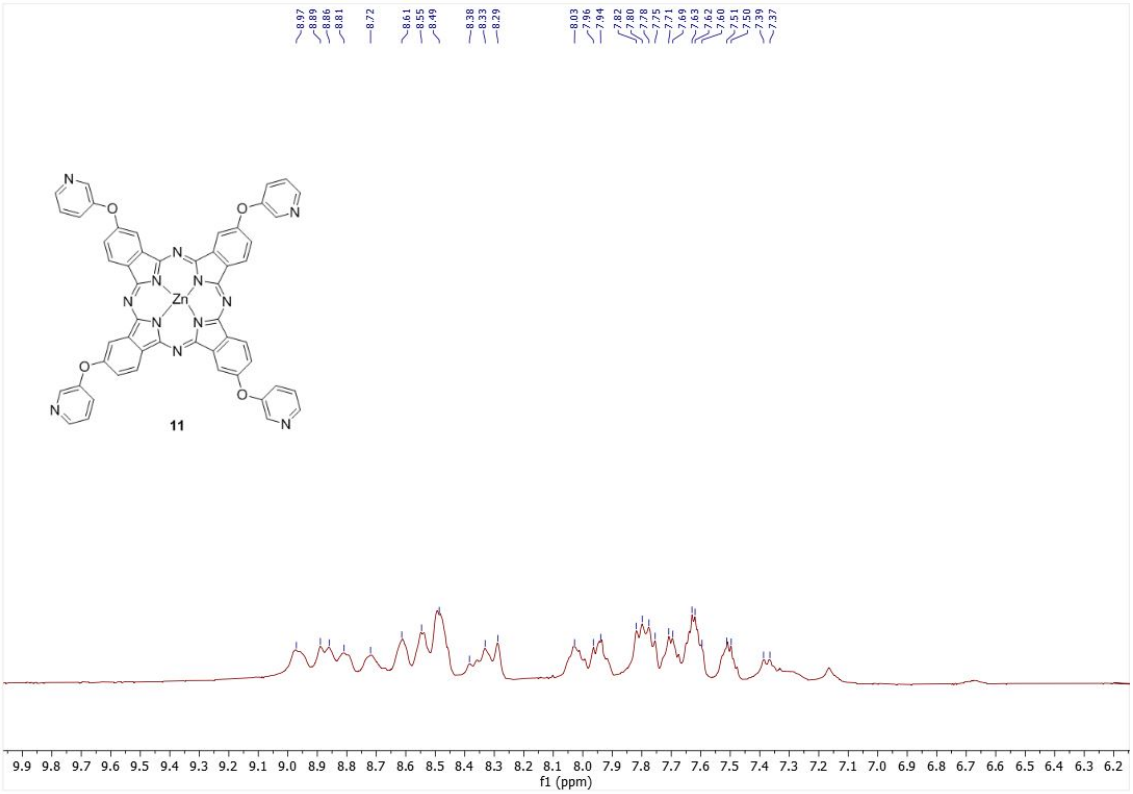

A23: ^{1}HNMR spectrum for compound **11**

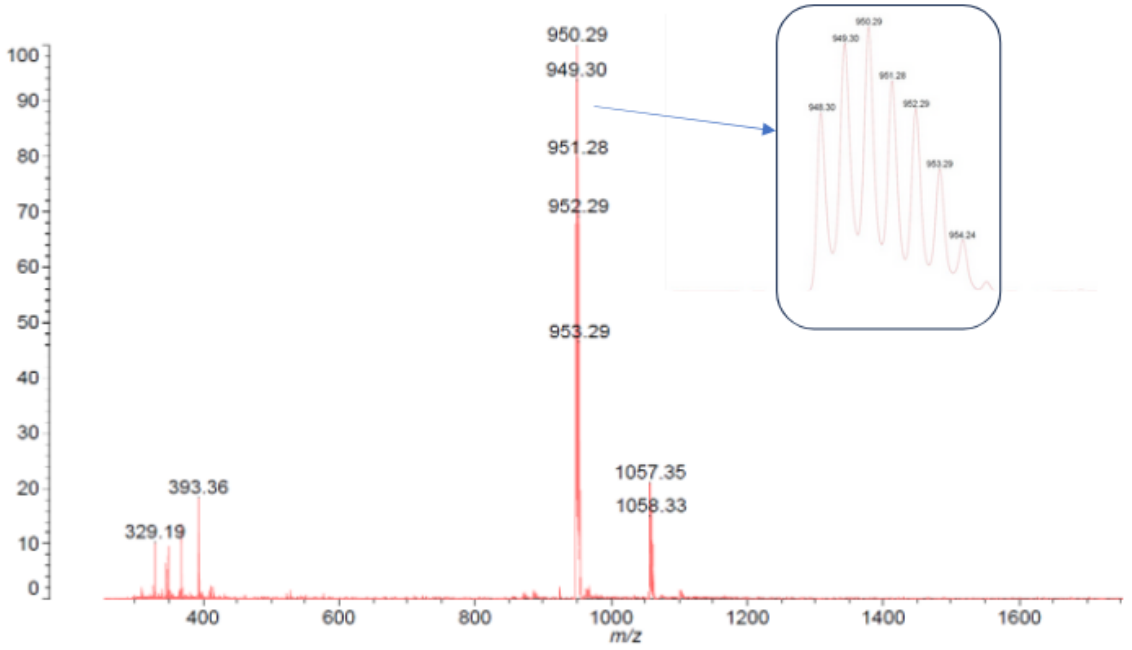

A24: MALDI-TOF spectrum for compound **11**

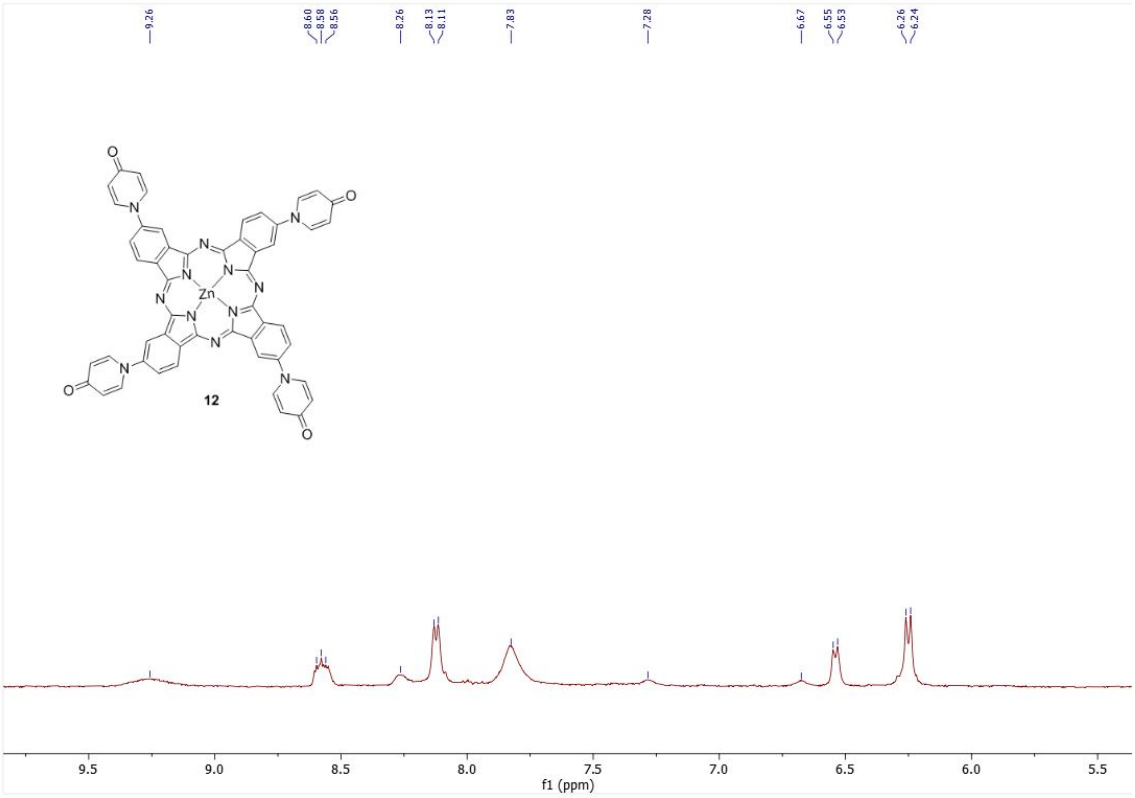

A25: ^{1}HNMR spectrum for compound **12**

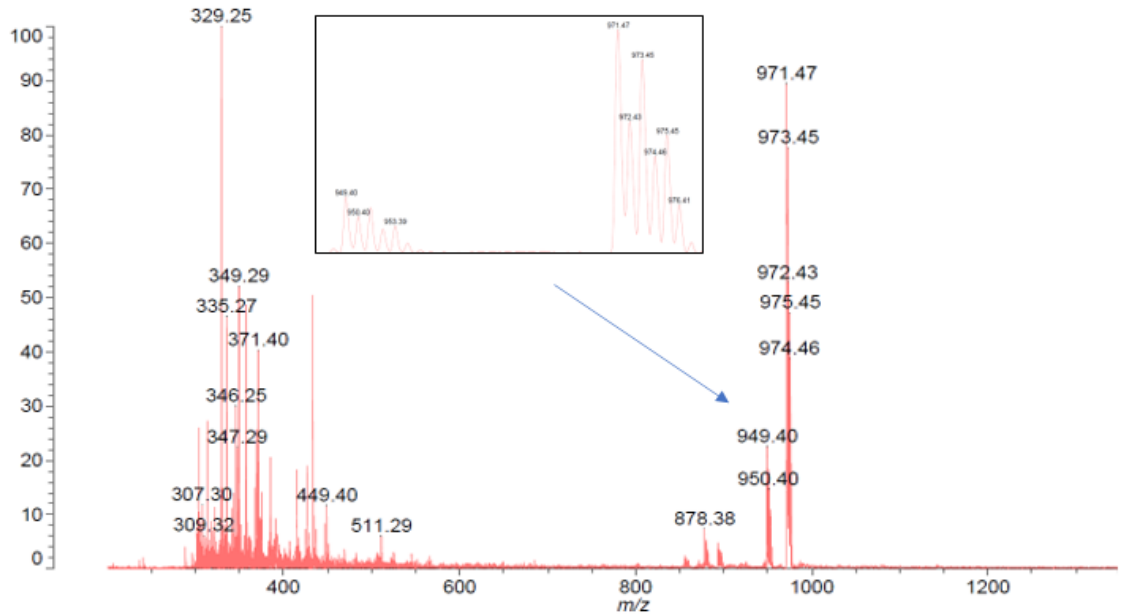

A26: MALDI-TOF spectrum for compound **12**

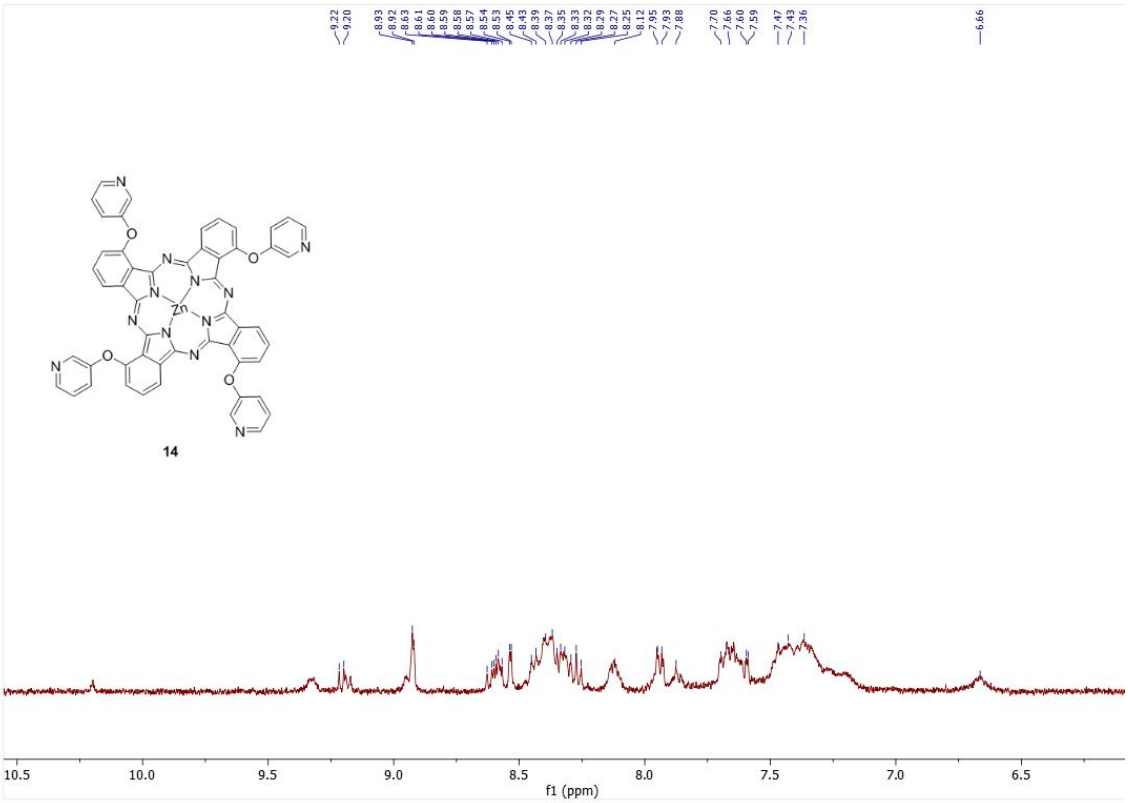

A27: [1]HNMR spectrum for compound **14**

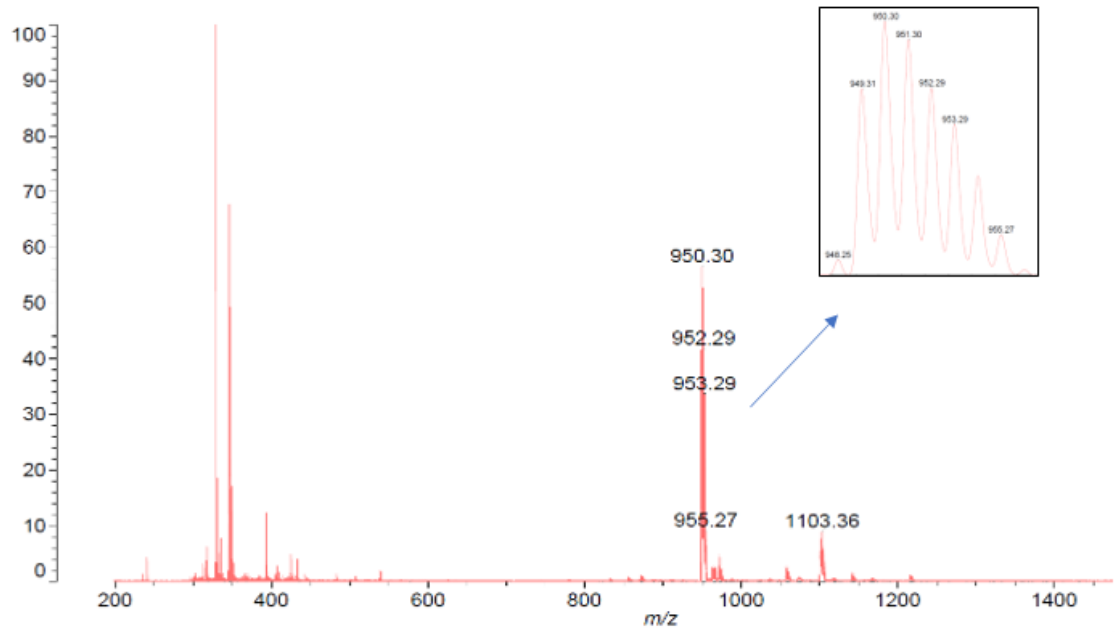

A28: MALDI spectrum for compound **14**

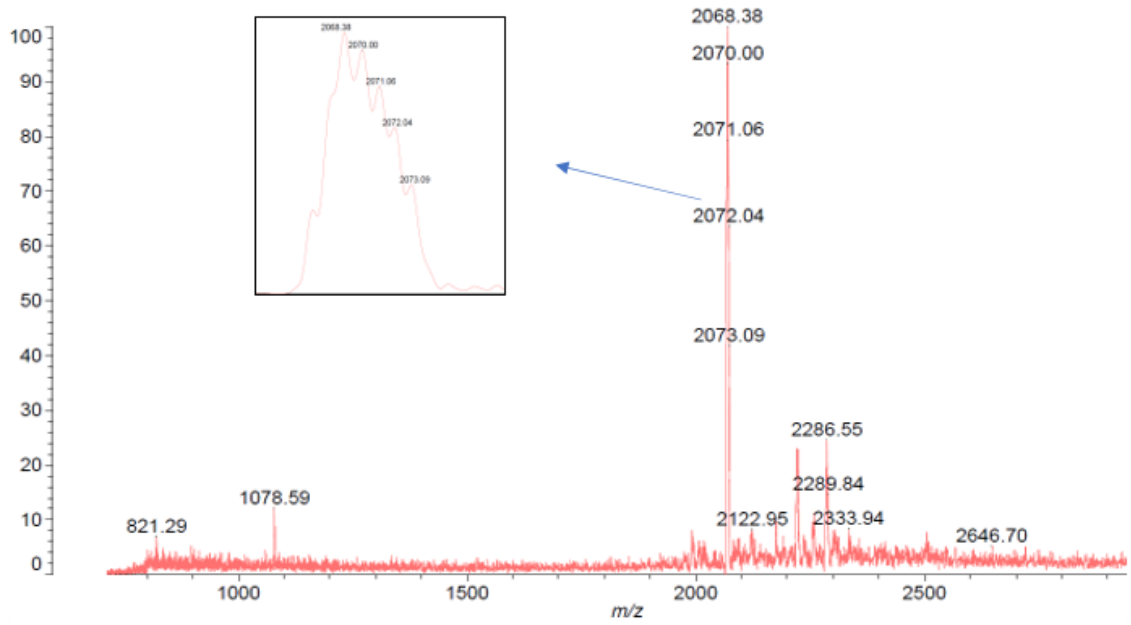

A29: MALDI spectrum for compound **15**